Influence of the design constraints on the thickness optimization of glass panes to achieve lightweight insulating glass units in cruise ships

Marine Structures 89 (2023) 103409

Contents lists available at ScienceDirect

Marine Structures

journal homepage: www.elsevier.com/locate/marstruc

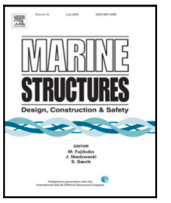

Influence of the design constraints on the thickness optimization of glass panes to achieve lightweight insulating glass units in cruise ships

Janne Heiskari [a,*], Jani Romanoff [a], Aleksi Laakso [b], Jonas W. Ringsberg [c]

[a] Department of Mechanical Engineering, Aalto University School of Engineering, Espoo, Finland
[b] Meyer Turku Oy, Turku, Finland
[c] Department of Mechanics and Maritime Sciences, Chalmers University of Technology, Gothenburg, Sweden

ARTICLE INFO

Keywords:
Insulating glass unit
Particle swarm optimization
Cruise ship design
Nonlinear finite element analysis
Classification
Load sharing

ABSTRACT

The increasing complexity and size in cruise ships demands for lightweight structures and practical but accurate design methods. Conventionally, the focus has been on the steel parts of the ship, as they make most of its weight. However, the proportions of other materials are increasing. Therefore, this study attempts to provide better understanding how one could reach the lightweight designs of insulating glass units (IGUs) in ships. These are windows where at least two glass panes are separated by a hermetically sealed cavity. They are thin-walled structures that benefit not only from the geometrically nonlinear behavior, but also from the load sharing. Considering these effects, their behavior is studied using the nonlinear Finite Element Method and Particle Swarm Optimization. Different design criteria are imposed on the thickness determination of the glass panes with different shapes. Rectangular, triangular, and circular shapes are considered. The results show that the triangular shapes have the least weight for a given area when the deflection criterion is the dominating one. When maximum principal stress is the thickness defining criterion, the shapes perform almost equally well. The ratio between the pane thicknesses had the most influence on the behavior of the IGU. As it increases, i.e., one pane is significantly thicker than the other, the load sharing percentage drops, but it provides the most lightweight solution. Closer it is to 1, more equally the structural stresses are divided between the panes, i.e., redundancy is achieved. Finally, it is possible to establish a simple but effective method for the thickness determination of these IGUs using the results of this study. However, more work is required, including numerical analysis and experimental testing.

1. Introduction

Cruise ships are growing in size and complexity to accommodate more on-board activities and features for the passengers. One inevitably consequence for this is the increased structural weight. Because managing weight and maintaining good stability is important for the ships, a lot of research has been conducted for achieving lightweight steel structures (e.g., [1–3]). At the same time, a focus is kept in developing methods that serve the designers in a practical manner and provide accurate response of the complex structure at the desired level of interest (e.g., [4]). Now, the increasing trend in cruise ships is to use more windows to allow the passengers to better enjoy the surrounding environment through glazed areas. That is, the sides of the ships are covered

* Corresponding author.
E-mail address: Janne.Heiskari@aalto.fi (J. Heiskari).

https://doi.org/10.1016/j.marstruc.2023.103409
Received 10 November 2022; Received in revised form 18 February 2023; Accepted 21 February 2023
Available online 28 February 2023

Fig. 1. Examples of insulating glass units in cruise ships. (A) and (B) are from Mein Schiff 2, and (C) is the Aqua Dome of Icon of the Seas. *Source:* Courtesy of Meyer Turku Oy.

with large windows e.g., in restaurants, lounges and other common areas (Fig. 1 A), and in cabins (Fig. 1 B). Such large cut-outs produced by the windows have been studied in the global response of the ship [5]. However, this global response is not affected by the window panes [6]. This could possibly be one of the reasons why the windows themselves have not received so much attention. Some studies of the ship windows exist, e.g., experimental and numerical analysis of the failure prediction [7], but not from the design point of view, similarly as has been done for the steel structures. Therefore, it has become of an interest to extend the lightweight requirement and the practical design aspects to the ship glass structures.

The considered glass structures in this study consist of insulating glass unit-type (IGU) of windows. They are used to provide thermal insulation, which is achieved by building the IGU from at least two glass panes that are separated by a hermetically sealed cavity. That is, the IGUs separate indoor and outdoor spaces. The cavity is often filled with some inert gas, like Argon, to enhance the insulation properties. Structurally, the IGUs exhibit a beneficial interaction of the glass panes, known as load sharing. When the outer glass pane (exposed pane) is subjected to an external loading, its deflection causes the volume of the cavity to decrease. According to the ideal gas law ($pV = nRT$), the pressure of the cavity increases, which in turn causes the inner glass pane (unexposed pane) to deflect; the load is shared. If the cavity leaks, moisture will be absorbed that will appear as a fog on the glass surfaces, which is a visual impairment. Such impairments will be noticed and repaired on cruise ships. For this reason, we argue that it does not pose significant additional risks when including the load sharing effect in the design process. The load sharing has been recently studied experimentally [8], analytically [9], and numerically [10]. The influence of the *load sharing* in conjunction with the *geometric nonlinearity* on the thickness determination of rectangular glass panes in the IGUs was studied numerically in [11].

There, it was shown that the considered effects reduce the stresses in the glass panes, which allows for choosing thinner panes. Reducing the pane thickness even by a few millimeters can have a significant overall weight reduction considering the amount of IGUs in the ship. The thickness comparison was made to the rules given by the classification societies (e.g., DNV [12]). The rules are generalized for all types of ships, which ensures sufficient load bearing capacity for the windows. The rules are based on linear plate theory and neglect the load sharing effect (see Appendix A). It was shown in [11] that this conservative approach leads to unnecessarily heavy IGUs. This might seem insignificant for cargo ships with very few IGUs. However, in cruise ships the total area of IGUs can be several thousands of square meters enabling significant weight saving potential. In the numerical study [11], however, the only considered design criteria was the maximum principle stress criterion, which was set to 40 MPa as per the classification rules. As a consequence, the used FE model resulted in rather high deflections even though the stress was within acceptable limits.

Such deflections can potentially cause aesthetical issues, risk the integrity of the sealing system of the IGU or cause feeling of unsafety to the passengers. Therefore, a study was conducted in [13] where two different deflection criteria were imposed on the FE model of the IGU in a Particle Swarm Optimization (PSO). Since there are no rules for the maximum deflection of the windows, limits of $L/100$ and $L/175$ were tested to see how they reflect on the weight optimization as limiting the deflection could be important in the future when more advanced thickness determination methods are used. The results indicated that the thicknesses are sensitive to the chosen deflection criterion. That is, relatively small increments of the limit significantly increase the thickness. The $L/175$ limit resulted in thicker constructions than suggested by the classification rules. The $L/100$ limit allowed good weight savings. Hence, by expanding the design limits beyond the classification rules, lightweight solution was achieved without harming the structural safety. However, the optimization was done only for rectangular panes with equally thick panes. The real IGUs in ships are not limited to these cases.

Therefore, those limitations are removed in this paper and different design criteria are imposed in calculating the required minimum thickness of the IGUs with various shapes. Rectangular ($a/b = 1$, $a/b = 1.25$, $a/b = 1.67$), triangular (right angle and equilateral), and circular shapes are considered. Circular IGUs are used in portholes, while triangular IGUs are common for creating large glass domes or other structures with curved surface, see Fig. 1 C. On the other hand, rectangular IGUs are often found in glass walls between the decks. Hence, this study also aims to provide insight on how to achieve the lightweight requirement for the IGUs and how the different criteria affect these results. For this, the same FE model is used as in [11,13] with the PSO algorithm, implemented in MATLAB. Once the response is known, it is possible to find which design criteria has been activated, i.e., which one is limiting the thickness. The resulting thicknesses are compared to the classification rule suggested method to demonstrate

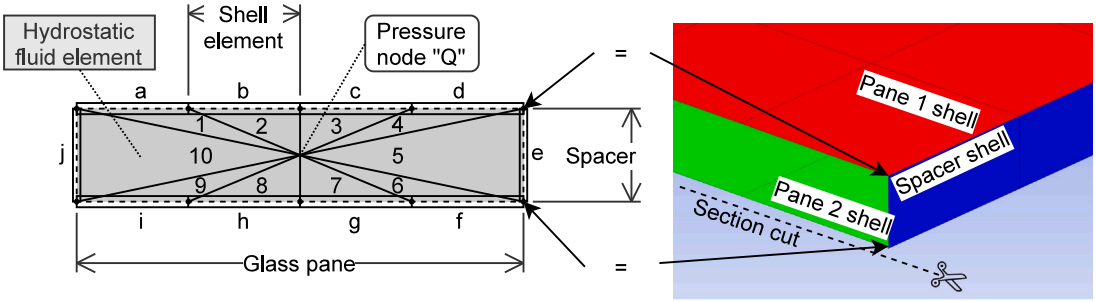

Fig. 2. Illustration of IGU model cross-section on the left-hand side. Letters and numbers represents the structural shell elements and hydrostatic fluid elements, respectively. The dashed line is the mid-plane of the shell elements. Gray colored area is gas. A section cut of the meshed model in ANSYS on the right-hand side (HSFLD242 element not visible).

how they reflect to the classification rules. Furthermore, to have a more realistic comparison, the class rule constructions are not assumed equally thick, like done before in [11,13]. A secondary goal is to find if an easy and fast alternative method is possible for the thickness determination of these elementary shapes. The analyzed IGUs in this study are considered to be of monolithic glass panes subjected to quasi-static loading. That is, laminated glasses[1] and dynamic loading are studied in the future, as both are highly present in ships. Further, the effect of variation in ambient temperature and pressure, i.e., the climate loads [14–16], and their combined effect with an external load on the response was studied in [17]. There, the maximum stress increased approximately by 12% due to the climate loads as per DIN 18008-1 [18] (omitting altitude change component), which should be considered when analyzing real IGUs. However, the climate loads are neglected in this study to limit the number of cases.

2. Methods

The finite element model of the insulating glass unit is presented first. The model and the analysis follow the procedure presented in [11]. ANSYS Mechanical APDL is used. The finite element method is convenient as it is applicable for various IGU constructions, including different glass pane shapes, loading conditions, boundary conditions, and other assumptions. Furthermore, the interaction of the panes is embedded in the model, and since a nonlinear analysis is performed, the effect of the geometric nonlinearity (von Kármán strains) on the internal pressure generation is automatically considered. As opposed to a method where the internal pressure is first solved with a linear analytical method, and the response of the panes is solved with nonlinear FE method separately. The latter approach underestimates the internal pressure of the IGUs that undergo large deflections [11]. For these reasons, the former method is preferred. Then, the FE model is integrated into a MATLAB Particle Swarm Optimization routine.

The PSO is chosen as it is applicable for various types of problem. One of its strengths is that it only requires the objective function value, i.e., gradient information is not required. Further, it can handle multiple design variable and constraints efficiently. Therefore, it is a powerful algorithm for engineers, e.g., in optimizing weight of ship structures [19,20]. The basic principle of the PSO and the applied design constraints are presented after the FE model.

2.1. Finite element model

The insulating glass unit finite element model consist of two glass panes, a hermetically sealed cavity, and four spacers. The spacers create the insulating cavity volume, but they are not structurally considered in the analysis. Ideally, they would be considered as they provide stiffness to the structure [21]. However, neglecting the additional stiffness is a conservative and practical approach. Moreover, the spacers are part of the detail design phase. The glass panes are modeled with 4-node SHELL181 elements that are governed by the First-order shear deformation plate theory, which includes the transverse shear deformation. This is, however, negligible for compliant panes (large and thin). The air in the cavity, or the gas, is modeled with 5-node HSFLD242 elements that are governed by the ideal gas law ($pV = nRT$). The elements and an illustration of the model cross-section are shown in Fig. 2. The mesh size is 50×50 mm^2 and 50×20 mm^2 for the glass panes and for the spacers, respectively. This model with the same mesh was validated in [11]. Therefore, no mesh convergence analysis is performed.

A nonlinear static structural analysis is conducted that follows the Newton–Raphson procedure. The outer glass pane, also referred as the exposed glass pane, is subjected to uniformly distributed pressure, $\bar{p}$. The four IGU edges (8 glass pane edges) are bounded so that only the translation normal to the glass pane is restricted. That is, the edges are allowed to move in in-plane and to rotate freely. However, the central nodes of the both panes are fixed in the in-plane to prevent rigid body motion. This represents a realistic and conservative approach that shows good agreement with the experimental results by McMahon et al. [8]. See Fig. 3 for the boundary conditions and comparison of the numerical results with the experimental results. It should be noted that this is conservative in

[1] Laminated glasses are formed by gluing together at least two monolithic glass panes by a polymeric interlayer. For laminated glasses, the classification rules allow for collaboration of the glued glass panes, which is in the favor of lightweight design.

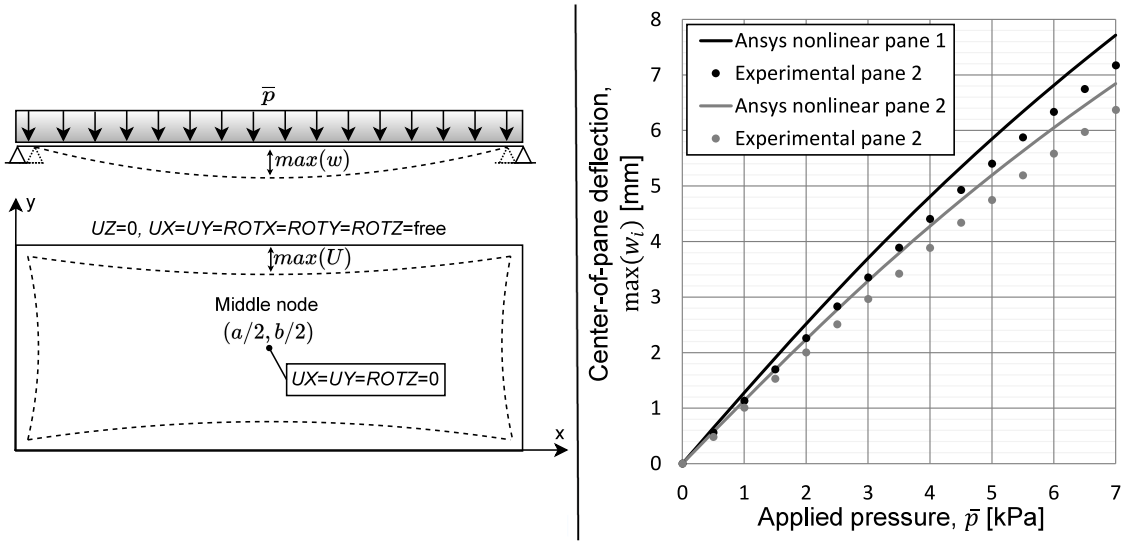

Fig. 3. Boundary condition and the corresponding deformed shape (exaggerated) for a rectangular shape on the left-hand side. Maximum deflection, $max(w)$, and maximum in-plane translation of the edge, $max(U)$, are as presented. The edge conditions are equal for both of the panes. Central nodes of the both panes are constrained for preventing rigid-body motion. On the right-hand side is center-of-pane deflection versus applied pressure for both panes of a rectangular IGU (a = 1260 mm, b = 750 mm, $t_1 = t_2$ = 5.7 mm, s = 13 mm), a comparison between finite element results [11] and experimental results by McMahon et al. [8].

terms of the deflections. If the rotations of the edges would be fixed, large normal stresses are generated on the top surface of the glass pane in the edge vicinity. However, since the IGUs are typically bonded, and not clamped, it is not realistic to assume fixed rotations. Further, such condition would significantly hinder the generation of the deflection, which results in large disagreement with the experimental results.

2.2. Particle swarm optimization

The swarm consists of a certain number of particles, which are denoted with an index i. The best swarm size is dependent on the problem. A swarm size of 150 is chosen to have computational efficiency, since the finite element analyses are highly nonlinear, even though generally a much larger swarm (up to 500) has been found to perform better [22]. Every particle in the swarm has two vectors; a position vector $\vec{x}_i(l)$ and a velocity vector $\vec{v}_i(l)$. The former describes the particle's current location in the domain at each iteration (l) while the latter describes in which direction the particle is moving and how much (magnitude). Each particle has a memory of its personal best position, $\vec{P}_i(l)$, at any iteration. Furthermore, each particle in the swarm keeps track of the global best position, $G(l)$, at any iteration. Each particle also has a j index that is dependent on how many design variables are used. For example, j is two when the thicknesses of the both panes are variables, i.e., the optimization problem is 2-dimensional. With these four parameters, a new velocity and a position is calculated for each particle in the next iteration, respectively, as:

$$\vec{x}_i(t+1) = \vec{x}_i(t) + \vec{v}_i(t+1) \tag{1}$$

$$\vec{v}_i(t+1) = w\vec{v}_i(t) + r_1 c_1 \left[\vec{P}_i(t) - \vec{x}_i(t)\right] + r_2 c_2 \left[G(t) - \vec{x}_i(t)\right] \tag{2}$$

where the first term is the *inertia term*, the second term is the *cognitive component* and the last term is the *social component*. The former term describes how wide the particle searches the domain. The latter two terms describe how much the particle trusts itself and how much it trusts the swarm, respectively. Further, r_1 and r_2 are random numbers with interval of 0 and 1. In the beginning, the initial positions and velocities are randomly generated, and the corresponding objective functions are evaluated. Now, the first particle best and global best positions are obtained. At each iteration, the particle moves some distance in the direction of current velocity, then in the direction of personal best, and finally in the direction of global best (Fig. 4). If the new position is better than the personal best, it is overwritten. The same applies for the global best. Hence, the PSO effectively searches the domain for the optimum at each new iteration. The acceleration coefficients c_1 (personal) and c_2 (social), and the inertia coefficient w are:

$$\begin{aligned} c_1 &= \chi\phi_1 \\ c_2 &= \chi\phi_2 \\ w &= \chi \\ \chi &= \frac{2\kappa}{|2 - \phi - \sqrt{\phi^2 - 4\phi}|} \\ \phi &= \phi_1 + \phi_2 \end{aligned} \tag{3}$$

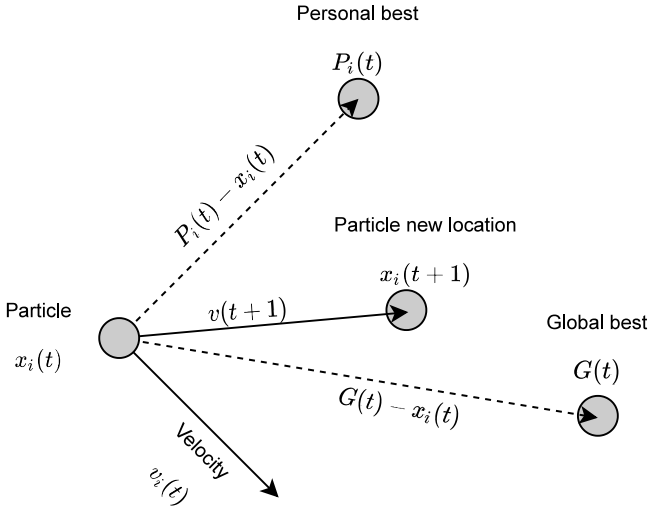

Fig. 4. The working principle of particle swarm optimization; determination of the new particle position.

where $\kappa = 1$, $\phi_1 = 2.05$, and $\phi_2 = 2.05$. Further, no damping of the inertia coefficient is used. However, the velocities are limited statically at each iteration as:

$$\begin{aligned} Velocity_{ij,max} &= \frac{Variable_{ij,max} - Variable_{ij,min}}{c} \\ Velocity_{ij,min} &= -Velocity_{ij,max} \end{aligned} \tag{4}$$

where maximum and minimum values are set for the variables, and $c = 5$. The purpose of limiting the velocity is to ensure that the particles do not take too large leaps in the search domain. Multiple studies exist how to improve the efficiency of the PSO (e.g., [23,24]), but the aforementioned procedure and parameters are sufficient for this study.

The purpose of the optimization routine is to minimize weight of the glass panes in the insulating glass units without breaking the design constraints. Since only double insulating glass unit is considered (two glass panes), the objective function is:

$$Minimize \qquad M(t) = \sum_{j=1}^{2} t_j A \tag{5}$$

where t_j are the thicknesses of the panes and A is the area of the panes. The objective function is limited by certain constraints:

$$\begin{aligned} &\sigma_+ \leq \sigma_{+,d} \\ &\delta \leq \frac{a}{\delta_d} \\ &U \leq U_d \\ &1 \leq \frac{t_1}{t_2} \leq r \\ &t_{lower} \leq t_{1,2} \leq t_{upper} \end{aligned} \tag{6}$$

where σ_+ is the maximum principal stress, δ is the deflection, U is the in-plane movement of the edges, r is the thickness ratio limit, *lower* and *upper* subscripts indicate limits for the glass pane thicknesses, and subscript d indicates the design values, which are defined later. Each of the response value (e.g., deflection) is evaluated with its corresponding criterion to check if they are met. Since the thicknesses are unequal, the response is checked from both of the panes (subscripts 1 and 2):

$$\begin{aligned} \eta_{c1} &= \frac{max\left[max(\sigma_{+,1}), max(\sigma_{+,2})\right]}{\sigma_{+,d}} - 1 \\ \eta_{c2} &= \frac{max\left[max(\delta_1), max(\delta_2)\right]}{\delta_d} - 1 \\ \eta_{c3} &= \frac{max\left[max(U_1), max(U_2)\right]}{U_d} - 1 \end{aligned} \tag{7}$$

where *max* is the maximum obtained value. Once the analysis is complete, the maximum eta-value is checked:

$$\eta = max[\eta_{c1}, \eta_{c2}, \eta_{c3}]. \tag{8}$$

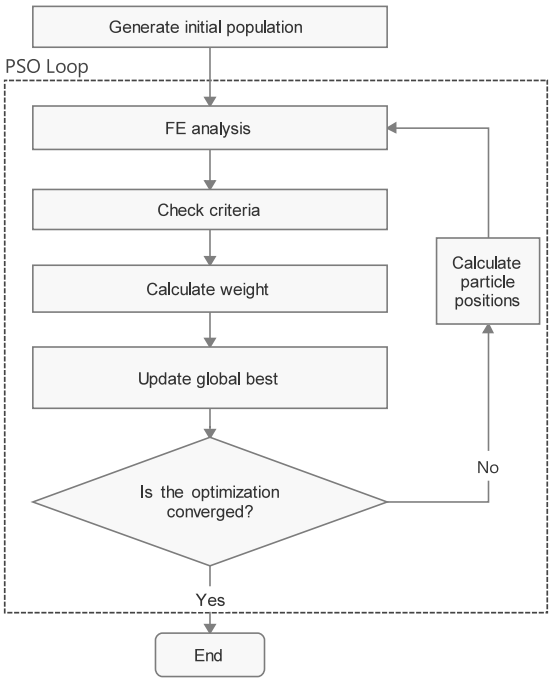

Fig. 5. Flowchart of the optimization routine.

If η is negative, the candidate is feasible and the corresponding weight is calculated. This is the objective function value. If η is positive, the candidate is unfeasible and the corresponding weight is calculated but a penalty is added. That is, more weight is added to this candidate so that it does not proceed as feasible:

$$M(t) = \begin{cases} \sum_{i=1}^{2} t_i A, & \text{if } \eta \leq 0 \\ \sum_{i=1}^{2} t_i A(1 + 100\eta), & \text{otherwise.} \end{cases} \tag{9}$$

When the objective function value (weight) has not improved in 4 consecutive iterations, the algorithm is stopped. The PSO routine is implemented in MATLAB and is described in Fig. 5.

3. Case study

In this chapter, the PSO routine is implemented in a MATLAB routine that runs the FE analyses. The thicknesses of both panes are varied while the IGU shape and size is kept constant. Once the optimum is found for that case, the size is increased, and the shape is changed, and so on until all the cases are optimized. Then, the weight of each optimized IGU is calculated, and a weight vs. area comparison is presented. This gives an idea if one of the shapes has the largest area with the least weight. To identify why a particular shape performs better than the other, a comparison of activation of the design criteria is made. That is, which criteria is limiting the thickness. The optimized thicknesses are then compared to the classification rules suggested design method. Finally, the developed stresses are studied in the optimized thicknesses and comments are given on the performance of the PSO algorithm. Only selected results are presented in the main text, while the rest are presented in Appendix B.

3.1. IGU dimensions and parameters

Six different IGU shapes are studied; (1) isosceles right triangle, (2) equilateral triangle, (3) square, (4) rectangle with $a/b = 1.25$, (5) rectangle with $a/b = 1.67$, and (6) circle (see Fig. 6). The area for each shape is (1) $\frac{a^2\sqrt{3}}{4}$, (2) $\frac{a^2}{2}$ (3) a^2, (4) $a \times b$, (5) $a \times b$, and (6) $\pi(\frac{a}{2})^2$, respectively. The characteristic length, a, is varied from 1000 mm to 5000 mm in intervals of 1000 mm. For the rectangular panes, the shorter side lengths are presented in Table 1. These aspect ratios are chosen to have a wider representation of the IGUs and they were able to provide good weight savings, as shown in [11]. However, there currently are not as large IGUs found in ships as presented in this paper, at least not to the authors' knowledge.

The physical parameters of the IGU are presented in Table 2. The density for the spacer and the glass are given as 0 to omit the effect of the self-weight. Its influence on the required minimum thickness for a square IGU with $a = 1500$ mm was verified to be small [11]. However, when non-vertically positioned real IGUs with large areas are designed, the self-weight should be included. The thickness of the spacers is chosen as 20 mm, which provides good thermal insulation, but is also commercially available. However, as the spacer thickness increases, the load sharing decreases [17]. However, for large and compliant glass panes, the decrease is not significant.

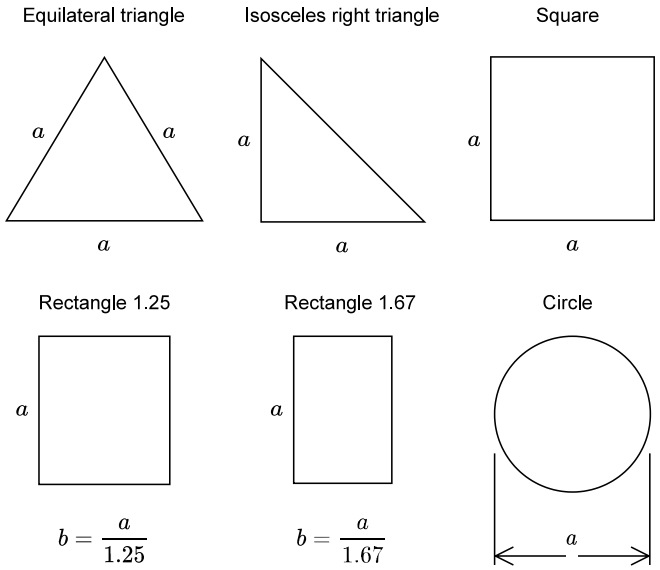

Fig. 6. Different IGU shapes.

Table 1
Rectangular IGU dimensions.

$a/b = 1.25$					
a [mm]	1000	2000	3000	4000	5000
b [mm]	800	1600	2400	3200	4000
$a/b = 1.67$					
a [mm]	1000	2000	3000	4000	5000
b [mm]	600	1200	1800	2400	3000

Table 2
Properties of the constituent materials.

	Glass	Spacer	Gas
E [MPa]	70000	0.01	0
ν [–]	0.23	0.01	0
ρ [kg/m^3]	0[a]	0[a]	1.7e−18[b]

[a]Self-weight not considered in the analyses.
[b]Numerical value required by the FE software.

3.2. Loading condition and response

Three different uniformly distributed loads are used; 2.5 kPa, 7.5 kPa, and 15.0 kPa. These are typical design loads used for ship windows located on the superstructure, deck sides or the aft. Closer the window is to the sea level, higher the design load is. The loads are considered to be quasi-static. The response consists of the maximum principal stress, maximum deflection, maximum in-plane translation of the edges, and the load sharing percentage. For the isosceles right triangle, the in-plane translation is taken in the direction normal to the hypotenuse. For all the other shapes, x- or y-direction is sufficient.

The load sharing percentage is calculated as ratio of the generated internal cavity pressure to the applied load ($p/\overline{p}\times 100\%$). If the directly loaded pane (exposed pane) is stiffer than the indirectly loaded pane (unexposed pane), then the load sharing percentage can reach up to 50%, which is the case in this study. However, if the unexposed pane would be stiffer (thicker) than the exposed pane, then the generated cavity pressure can be larger than the applied load, and hence the load sharing percentage can be more than 50%.

3.3. Design constraints

The design constraints are presented in Table 3. The classification rules only provide maximum principal stress criterion of 40 MPa. The glass panes should have at least 10 mm overlap with the mounting frame, or $b/75$, whichever is larger, but no more than

Table 3
Design constraints. For rectangular shapes, a is replaced with b.

Design constraint	Symbol	Value
Maximum principal stress	$\sigma_{+,d}$ [MPa]	40
Maximum deflection	δ_d [mm]	$a/100$ & $a/160$
Maximum in-plane translation	U_d [mm]	2
Thickness ratio limit	r [–]	3
Thickness lower limit	t_{lower} [mm]	4
Thickness upper limit	t_{upper} [mm]	varied

20 mm [12]. Since slipping of the pane from the mounting frame means loss of water-tightness, a strict limiting value of the in-plane translation of the edges is chosen as 2 mm. It has been shown in the previous studies that the panes experience similar deflections, and therefore it is not possible that the panes would get in contact with each other, at least not in quasi-static loading. Hence, it is not required to set the deflection difference of the panes as a constraint, like done in the previous study [13].

The lower limit for the pane thickness is chosen as 4 mm. The upper thickness limit is varied depending on the size of the glass pane and the applied load so that the optimization search domain is reasonable. It should be noted that continuous thickness values are used in the optimization, while in reality there are only certain standard thicknesses available. The thickness ratio is chosen so that t_1 must be always larger than t_2, but can be only 3 times larger; $r = 3$. The reason for r is to have reasonable constructions. Furthermore, it is intuitive decision for an IGU consisting of monolithic glass panes that the exposed pane is thicker than the unexposed pane, e.g., because class rules only provide thickness determination for the exposed pane. However, in applications where it is possible that broken shards can cause harm to the passengers, the unexposed pane must be of laminated construction. Such IGU construction is required e.g., in an over-head glazing structure. Then, the total thickness of the unexposed laminated glass can be thicker than the exposed monolithic glass pane.

Finally, choosing the deflection limits is not a trivial task, as the optimized thicknesses are sensitive to it. This was shown in [13] for rectangular IGUs for 2.5 kPa design load. There, limits of $b/100$ and $b/175$ were used, and the latter choice produced thicker glass panes than the classification rules would have. Therefore, slightly less strict limit of $a/160$ is chosen for this study in addition to the $a/100$ limit. The latter is sometimes used in ship steel structures. It should be noted that for the rectangular shapes, a is replaced with b. That is, the shorter side is used to calculate the limit. In the future, it is desired to experimentally study how the large deflections influence the functionality of the IGU. This includes the visual perspective (distortion), noise insulation properties, and integrity of the sealing systems in the perimeter of the IGU. Then, one can determine better how the limit should be chosen.

3.4. Optimized thicknesses

The resulting optimized thicknesses are presented first for all the shapes, sizes, and design loads. Since there are 3 design loads, 6 shapes, 5 sizes, 2 deflection limits, and 2 glass panes, the total number of thicknesses is 360. These are presented in Fig. 7. It is clear that the triangular shapes require the smallest thicknesses for a given side length. As the design load increases, the required minimum thickness grows for the circular pane with respect to the others. On the other hand, rest of the shapes maintain their "order", which is from the thinnest to the thickest: (1) equilateral triangle, (2) isosceles right angle triangle, (3) rectangle with $a/b = 1.67$, (4) rectangle with $a/b = 1.25$, and (5) square. Introducing to the stricter deflection limit only shifts up the required thickness. Across all the cases, the thicknesses are sometimes limited by the 4 mm minimum thickness criterion. This can be seen where the lines are horizontal in the beginning. Then the thicknesses increase linearly as the characteristic length increases. Therefore, one could in theory extract a simple linear equation from these graphs for each shape, load case, and deflection criteria, for determining the thickness of the panes.

This could be done for both panes or just for the one pane. The thickness of the other pane can also be calculated from thickness ratio. See Fig. 8. The limit for the ratio was set to 3, and indeed the optimum case is when the ratio reaches this number. That is, the lightweight solution is obtained when the exposed pane is about 3 times thicker than the unexposed pane. Achieving this thickness ratio for small loads and small or moderate sizes may be difficult, because the lower limit of 4 mm has been reached. As of now, typically the smallest thickness allowed is 6 mm, which further complicates achieving this ratio. However, a thickness of 4 mm is also possible, but probably requires experimental proofing of its structural integrity[2] or it must in laminated construction. Regardless, the optimization shows that the weight of the IGU decreases as the thickness ratio increases. This means that the exposed pane carries most of the load. This is further discussed in Section 3.8.

3.5. Weight vs. area comparison

The weight of the insulating glass unit is calculated considering only the glass panes with density of 2500 $\mathrm{kg/m^3}$. The results in Fig. 9 show that the triangular shapes perform best in all the cases except for the largest load with $a/100$ criterion. There, all the shapes are at the stress limit, i.e., the maximum principal stress is 40 MPa. Therefore, there is only small difference between the

[2] Dynamic pendulum test is required for glass panes in such locations where risk of people cutting or piercing themselves is possible, or where containment of material is required. The test is done according to EN 12600:2002 [25]. A four point bending test according to EN 1288-3 [26] may also be required.

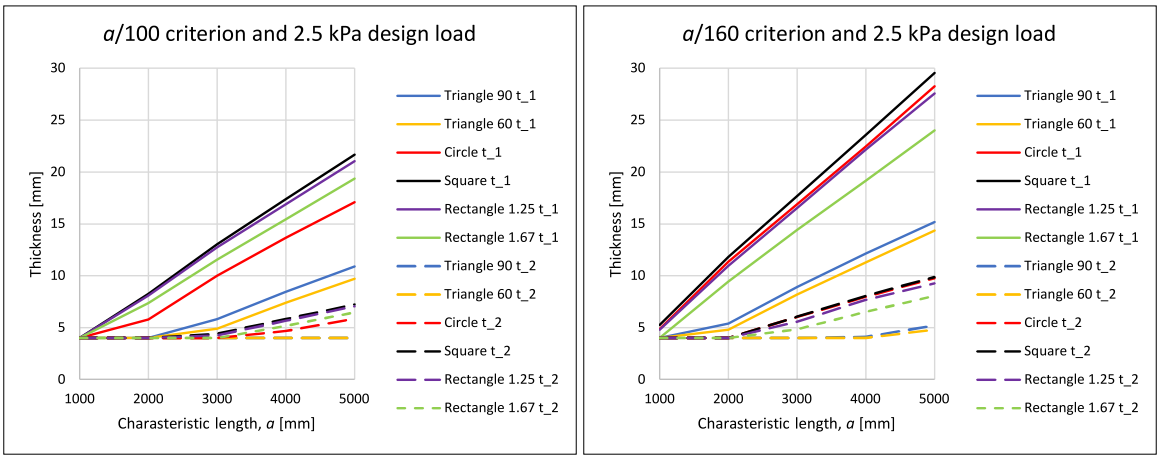

Fig. 7. The optimized thicknesses: t_1 and t_2 are for exposed pane and unexposed pane, respectively.

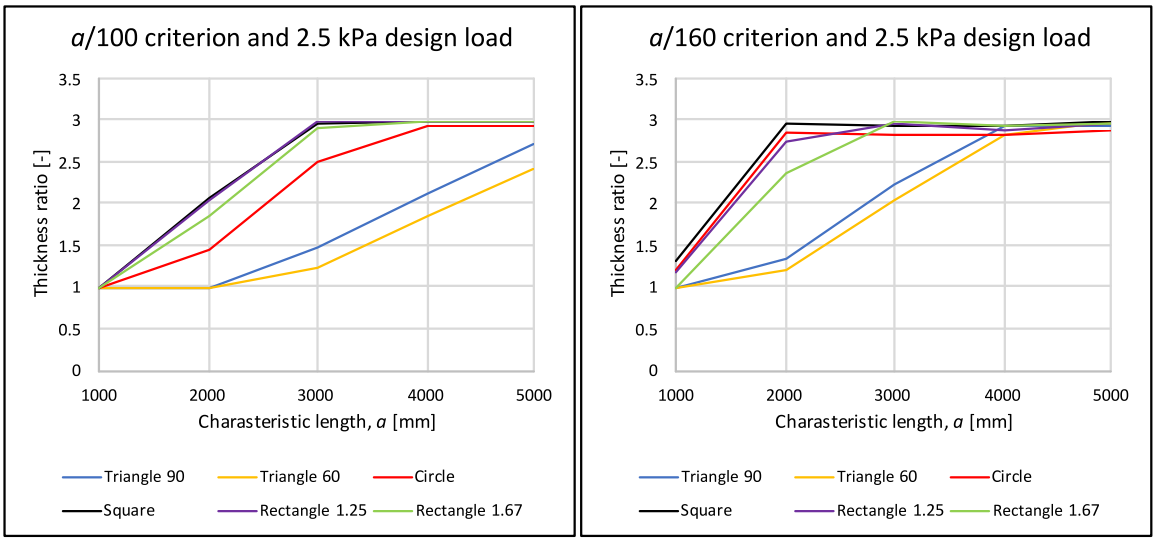

Fig. 8. The thickness ratio of exposed pane to unexposed pane for the optimized thicknesses.

shapes when using a large design load. This suggests that without any deflection limits, the shapes perform almost equally well. Increasing the deflection limit is in the favor of the triangular shapes, while there is no significant influence on the other shapes. For rectangular panes, it is widely known that aspect ratio $a/b = 1$ is the most efficient, which can be seen in all the loads and both deflection limits. That is, square always weighs less than the rectangles for a given area. The circular shape, however, performs better than the square for 2.5 kPa design load with $a/100$ criterion, but for the rest of the cases, square is more efficient. However, this comparison is only true for individual windows as it may be a better solution to use e.g., multiple rectangular IGUs instead of a fewer square IGUs, or multiple triangles instead of rectangles.

In that case, the weight of the supporting steel structure should be considered because square shape requires less supports in glass curtain walls or in domes as compared to triangular or rectangular shapes. For example, consider a wall with bottom width of $3a$ and height of a (see Fig. 10). It can be built from 4 different shapes while maintaining the same total area; (A) equilateral triangle,[3] (B) isosceles right triangle, (C) square, or (D) rectangle with $a/b = 1.67$. The required number of IGUs for each are 7, 6, 3, and 5, respectively. Extracting the weights from Fig. 9 for each $a = [1000, 2000, 3000, 4000, 5000]$ mm, a comparison for this glass wall can be made. For example, for 2.5 kPa design load and $a/100$ deflection criterion, the accumulated weights are presented in Table 4. It is clear that the triangular IGUs are the most lightweight solution in terms of the glass weight. If the added weight from the steel support structure is considered, the (A) and (B) cases are still lighter than the (C) and (D) for $a = 3000, 4000, 5000$. The

[3] The height for this shape is $0.866a$ and the area expressed without digits only varies by 1 m^2 for $a = 5000$ mm.

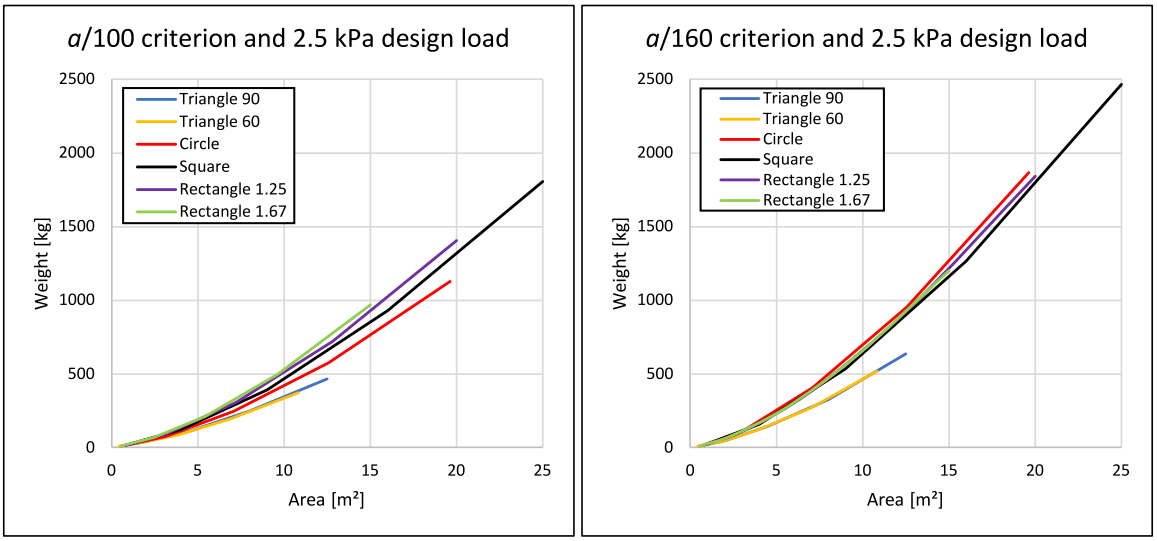

Fig. 9. Weight vs. area comparison of the optimized thicknesses.

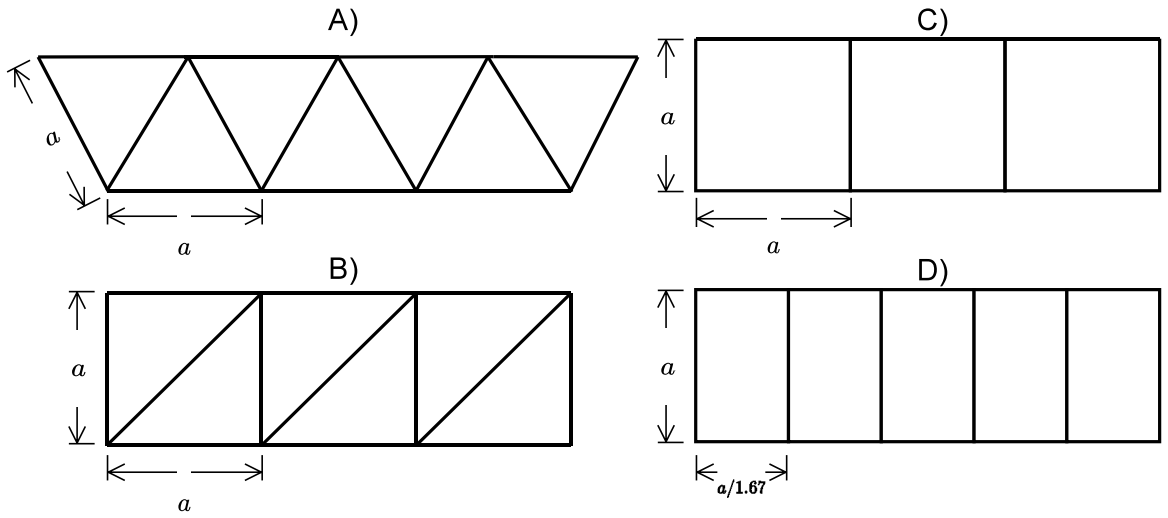

Fig. 10. A weight comparison example of a glass curtain wall built from different shapes; (A) equilateral triangle, (B) isosceles right triangle, (C) square, and (D) rectangle with $a/b = 1.67$. The total area is the same for all.

square is the lightest for $a = [1000, 2000]$ mm giving the considered RHS 200 × 100x8 mm profile as the support. In reality, the supports are also optimized, while this is merely a general demonstration. It should be noted that 4000 mm and 5000 mm windows are extremely large while 3000 mm is still large but can be currently found in some cruise ships. And for that size, the total weight difference between triangular and rectangular shape is between approximately 150 kg and 300 kg. However, the added support structures hinder the view. Therefore, choosing the window shape is also an aesthetical question.

3.6. Activation of design criteria

To find out which criterion is limiting the thickness, an η-value is plotted for each respective case. It is calculated as $\eta = response/criterion$. For example, if the maximum principal stress is 39 MPa, then $\eta = 39/40 = 0.975$. Hence, values of 1 mean that a particular criterion has been reached. See Fig. 11 for the results. Note that only the response of the exposed pane is presented.[4]

[4] The in-plane translation of the unexposed pane for some characteristic lengths and design loads can be slightly larger than of the exposed pane. However, they are still below the maximum criterion.

Table 4
Comparison of weights for a glass curtain wall subjected to design load of 2.5 kPa and $a/100$ deflection limit. A, B, C, D consist of 6, 6, 3, and 5 IGUs, respectively. The latter section includes the steel support structure (200 × 100x8 RHS profile with weight of 35 kg/m). The required supports in the added weight calculation are 6, 5, 2, and 4 for (A), (B), (C), and (D), respectively.

Weights including only glass				
a [mm]	A [kg]	B [kg]	C [kg]	D [kg]
1000	61	60	60	60
2000	242	240	368	341
3000	607	664	1179	1051
4000	1382	1494	2788	2476
5000	2595	2790	5416	4845
Weights including glass and steel				
1000	271	235	130	200
2000	662	590	508	621
3000	1237	1189	1389	1471
4000	2222	2194	3068	3036
5000	3645	3665	5766	5545

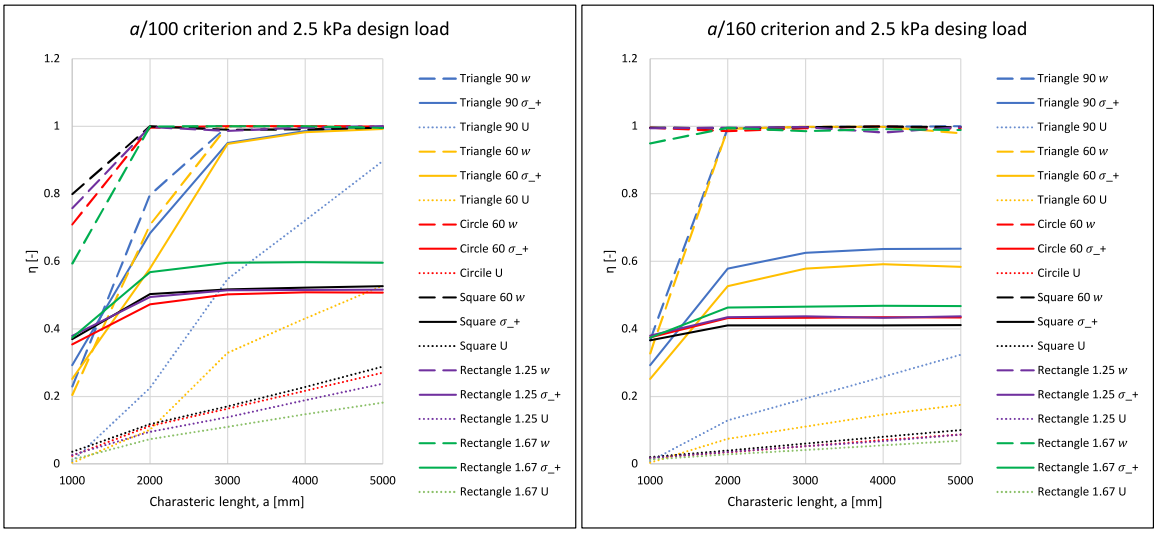

Fig. 11. Activation of the design criteria in the exposed pane. The activation is $\eta = response/criterion$. Value of 1 means that the criterion has been reached. U is the maximum in-plane translation of the edge and w is maximum the deflection as shown in Fig. 3, and σ_+ is the maximum principal stress.

The first observation is that the in-plane translation is not a limiting criterion in any of the cases. The limit is either the stress or the deflection, depending on the case. Secondly, when the deflection limit is changed from $a/100$ to $a/160$, the stresses reduce. The closer the stress is to the stress criterion, the lighter the IGUs are. The reason why triangular panes are so effective at 2.5 kPa design load and $a/100$ criterion is that both stress and deflection criteria are activated at the same time. Such condition can be called as "fully stressed design". Of course, this condition cannot be reached for the smallest sizes because the minimum thickness limit of 4 mm has been reaches. Obviously, the area of the rectangles and the circle are larger than the triangles with the same characteristic length, while their diagonal/diameter is also larger than the median of the triangles. Hence, it is intuitive that the deflection criterion is more dominant for all the other shapes than the triangles.

3.7. Comparison to classification rules

The optimized thicknesses are compared to the classification rules as per Appendix A. That is, the thickness of the exposed pane is calculated according to that. DNV [12] prescribes a minimum thickness of 6 mm or 8 mm for a glass pane located on the top structures with an area of less than 1 m^2 or more than 1 m^2, respectively. Hence, if the equations gives less than these for the exposed pane, it is disregarded. The second pane is always chosen as 6 mm or 8 mm, as this would be a more realistic approach done by the glass designers. The results are presented in Fig. 12. The smaller the load, size, and deflection limits are, the more savings can be achieved. This is partly due to the fact that in the FE routine minimum thickness of 4 mm is allowed, which creates a little bit of bias to the results in the favor of the FE method. On the other hand, for larger sizes with design loads of 7.5 and 15 kPa,

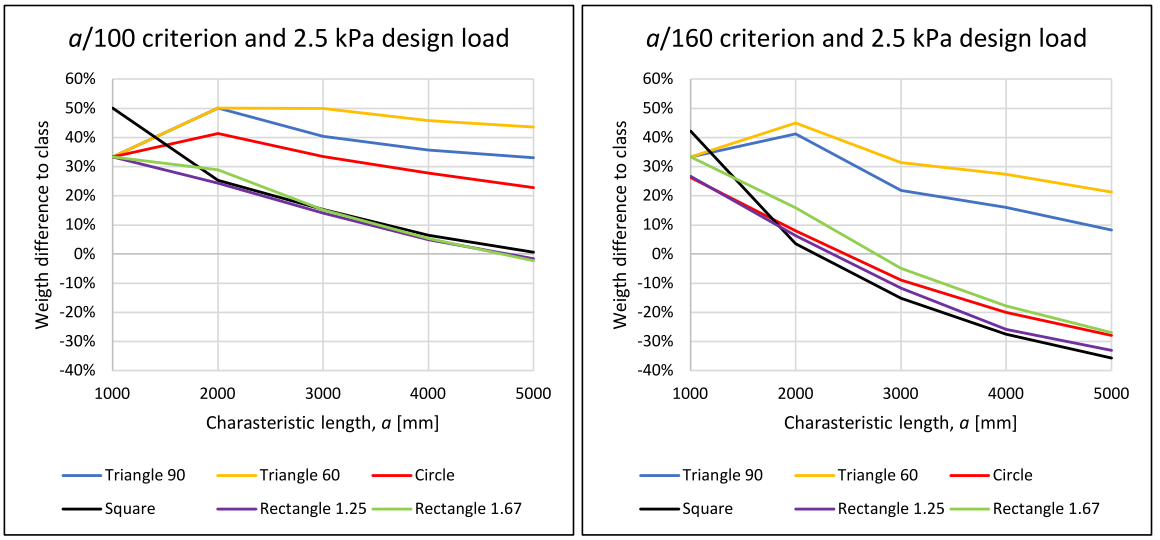

Fig. 12. Weight difference between the optimized thickness and the classification society method as per ISO 11336-1 [27]. The optimized thicknesses follow $t_1 \neq t_2$, while the classification thicknesses follow t_1 according to equations in Appendix A (minimum 6 or 8 mm), and t_2 is 6 mm if less than 1 m^2 or 8 mm otherwise.

the bias is on the classification rule method, since thickness ratios over 3 are produced. For example, with 15 kPa load and square IGU with $a = 4000$ mm, thicknesses are 41.3 mm and 8 mm for the exposed and unexposed pane, respectively, giving the aspect ratio more than 5. It is not clear if this would be admissible by to the classification societies.

Therefore, this kind of comparison is not so straightforward. However, the analysis demonstrates that the structural integrity of the IGUs is not harmed from the strength point of view when smaller thicknesses are used than prescribed by the class rules. Hence, results in Fig. 12 give some indication on the goodness of the considered methodologies. Across all the cases, the difference between the methods varies between −35% and 66%. Clearly, the triangular shapes provide the most savings. But even for those, the number goes to negative values, meaning class rules provide thinner solution, as the load and deflection limit are increased. This is because of the large thickness ratios. Without the thickness ratio restrictions, the FE model would provide thinner constructions for all the sizes and shapes. But with the considered ratio, moderate sizes (up to 3000 mm) and the smaller deflection limit, there are good savings available, especially for the 2.5 kPa and 7.5 kPa design loads. In fact, these represent the most common cases IGUs currently have in cruise ships; small design load and small to moderate size.

The minimum thicknesses 6 mm and 8 mm hinder the applicability of the classification rules to the lightweight solutions. Without those, say with 4 mm minimum thickness, the rule method would be quite reasonable for some cases. However, then one could not always choose it as the minimum thickness for the unexposed pane, as the results show in Section 3.4. Therefore, using advanced design methods where thicknesses of both panes are calculated are still suggested when searching for the true optimal solution.

3.8. Response ratio and load sharing

The response of the exposed pane was presented in the previous sections. Here, the response of the unexposed pane is presented using the response ratio. That is, the maximum principal stress and the maximum deflection ratios are calculated as the response of the unexposed pane over the exposed pane. If the ratio is 100%, then the panes have identical response values, while percentages close to 0 mean that the exposed pane has much larger values. See Fig. 13 for the results. Firstly, the deflection limit has only a small influence on the response ratio. It is clear that the panes experience similar deflections. However, the stress is quite different. For the highest design load, the stress ratio converges to around 30% to 40%. For the smallest load, the stress ratios are varying very much because the minimum thickness criterion has been reached for the small sizes. If the panes are equally thick, like for the small triangles, the ratios start to reach 100%. Hence closer the thickness ratio is to 1, more equally the stress is between the panes. If ratios smaller than 1 would be allowed, then it would be possible to reach stress ratios of 100%.

The same trend can be observed with the load sharing (see Fig. 14). When the thickness ratio is close to 3, the load sharing percentage is between 5% to 15% across all the shapes and design loads, and the two deflection limits. Clearly, the exposed pane carries more load than the unexposed pane. These results can be compared to results in [13], where the thickness ratio was 1. For example, consider a square IGU with $a = 3000$ mm subjected to 2.5 kPa design load and $a/100$ deflection limit. With thickness ratio of 1, the required thicknesses are $t_1 = t_2 = 9.7$ mm (as reported in [13]), while if the thickness ratio is 3, the required thicknesses are $t_1 = 13$ mm and $t_2 = 4.4$ mm. That is a 2 mm difference in total thickness (around 10%); latter option weighing less. That means a difference of 45 kg for a 3000×3000 mm square IGU. The load sharing percentage for the former is 49% while 8% for

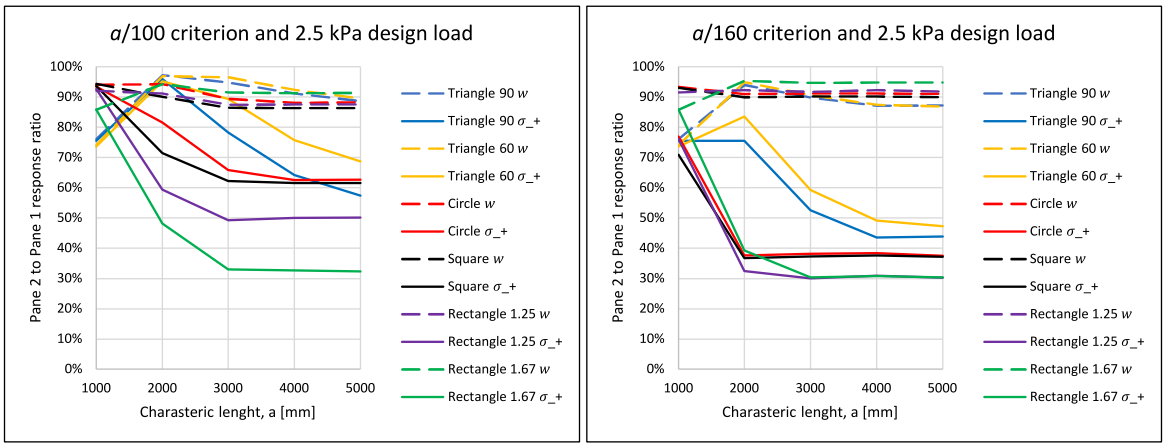

Fig. 13. The response ratio between unexposed pane (pane 2) and the exposed pane (pane 1). 100% means that the panes have identical response. σ_+ is the maximum principal stress, and w is the deflection.

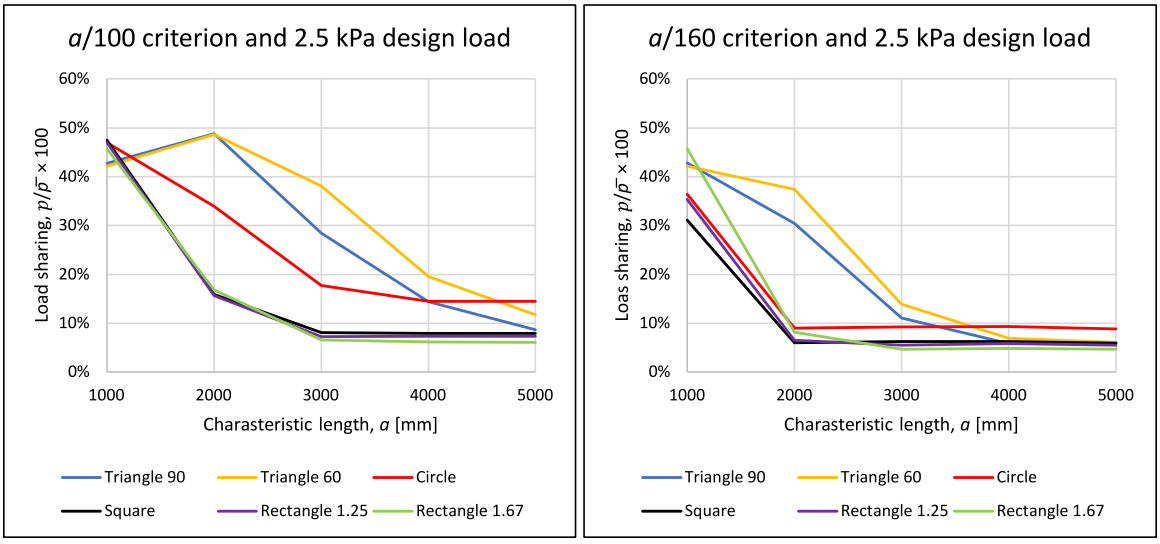

Fig. 14. Load sharing between the panes. It is calculated as the ratio of the pressure inside the cavity and the applied external pressure.

the latter. When the panes are equally thick, the stress ratio between the panes is 97% while it is 62% when the thickness ratio is 3.

The 10% difference show that having the glass panes equally thick is not a bad design, as long as their determination takes the load sharing and geometric nonlinearity in account. Equally thick panes also provide redundancy. Redundancy here refers to a case if either IGU glass pane would break by an accident, i.e., the load sharing is lost, the intact pane could most likely be able to carry normal design loads until repair. However, for further weight loss, it is recommended that the other pane is chosen thinner, but it does not have to be the unexposed pane that is thinner. Like mentioned earlier, if the unexposed pane is of laminated construction while the exposed is monolithic, then it is very reasonable to design the laminate package thicker than the monolithic pane. Then the load sharing percentage becomes higher than 50% (i.e., the cavity pressure is higher than the applied pressure) and the unexposed pane carries more load (being thicker). In the case where thickness ratio is high (e.g., 3), i.e., the other pane carries most of the load, and the thick glass pane would break by an accident, the remaining thin glass pane may not be able to carry the normal design loads on its own. Hence, redundancy is reduced.

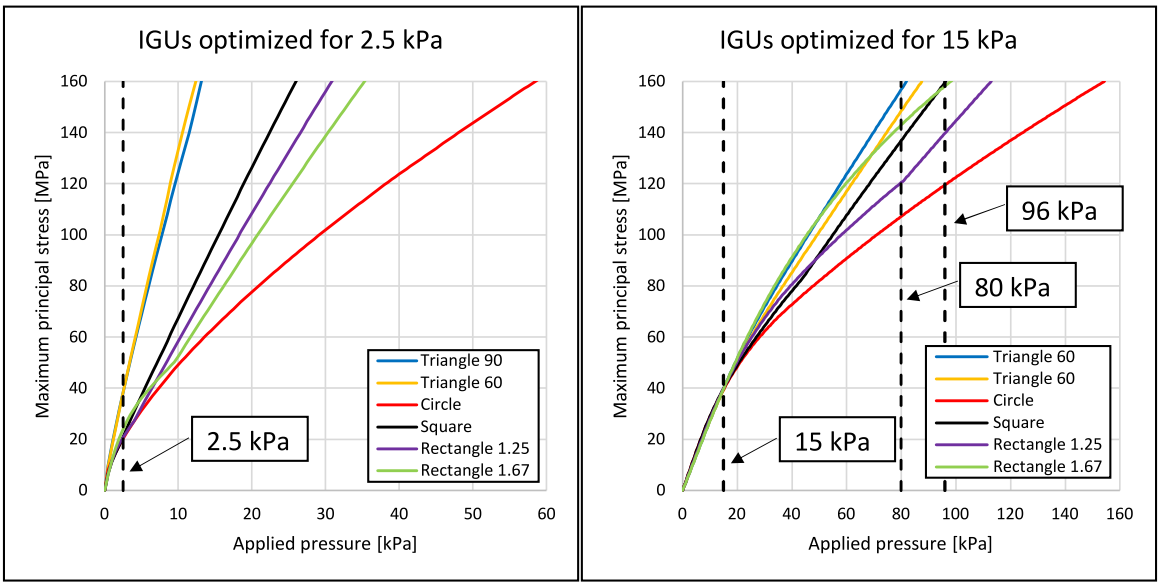

Fig. 15. Optimized IGUs loaded until stress of 160 MPa has been reached. The thicknesses are optimized for 2.5 kPa and 15 kPa design loads on the left-hand side and on the right-hand side, respectively. The corresponding design loads are represented with dashed lines. In addition, the load magnitudes representing dynamic loads used in [28] are also presented with dashed lines.

3.9. Estimation of durability against dynamic load

The ship windows may be subjected to dynamic loading due to wave impacts. The occurrence of such loads becomes more likely lower the windows are located. The magnitude of the loads can be very high. Design loads of 80 kPa and 96 kPa were used in [28], where the windows were tested experimentally and numerically against wave impacts. As mentioned, no dynamic analyses is performed in this paper, but the quasi-static analysis may be used to estimate how large loads the optimized IGUs can withstand until 160 MPa stress is reached, which is the characteristic failure strength of fully tempered glass without any safety factor (according to the classification societies and ISO 11336-1 [27]). Then, the corresponding loads can be compared to those used in [28]. The response of IGUs optimized for 2.5 kPa and 15 kPa design loads with $a/100$ deflection criterion are presented in Fig. 15.

Clearly, the IGUs can withstand much more than the design load with safety factor of 4. However, the ones optimized for 2.5 kPa design load cannot withstand the 80 kPa load. The circular and the triangular shapes can carry the most and the least load, respectively. The same is observed for the IGUs optimized for 15 kPa design load, except all the shapes can withstand the 80 kPa load. There, the circular shape reaches 160 MPa stress approximately at 150 kPa load, giving safety factor of 10 with respect to the original design load. However, it should be mentioned that glass does not have a single strength value. Hence, an individual window may or may not be able to withstand 160 MPa stress. If wave impacts are expected for the large IGUs, then they are probably of laminated construction. That is, the overall thickness will be automatically larger even if they are optimized. Then, the load carrying capacity grows.

3.10. The stress composition on the optimized thicknesses

The maximum principal stress contours are plotted for the exposed pane to find out where the maximum value is located. See Fig. 16 for the results. In linear analysis, it is typically in the geometric center. However, with nonlinear analysis and the given boundary conditions, its location cannot be determined intuitively. The bottom side of the pane is shown, where the maximum stresses are located. These are plotted only for one characteristic length, say $a = 3000$ mm, since there is no difference in the contours for a certain shape and deflection limit, when a is increased from 1000 mm to 5000 mm. The plots are made for each shape, design load, and both deflection limits.

The location of the maximum value of the maximum principal stress varies as the load is increased. More so for the $a/100$ limit than for the $a/160$ limit. In fact, the location is only moving for the triangular shapes for the latter. For both of the deflection limits, the location moves towards the center as the load is increased. Knowing where the maximum principal stress is located can be important when inspecting for surface defects. Further experimental tests will give more information if this theoretical location of the starting point for the failure is true or not. However, one should remember that 40 MPa is still far away from the failure strength of fully tempered glass. Hence, the location could still move after 40 MPa has been reached. This figure also shows that the stress becomes higher as the load is increased, which was already observed earlier in Fig. 11. Furthermore, it highlights how the triangular shapes enjoy higher stress levels than the other shapes.

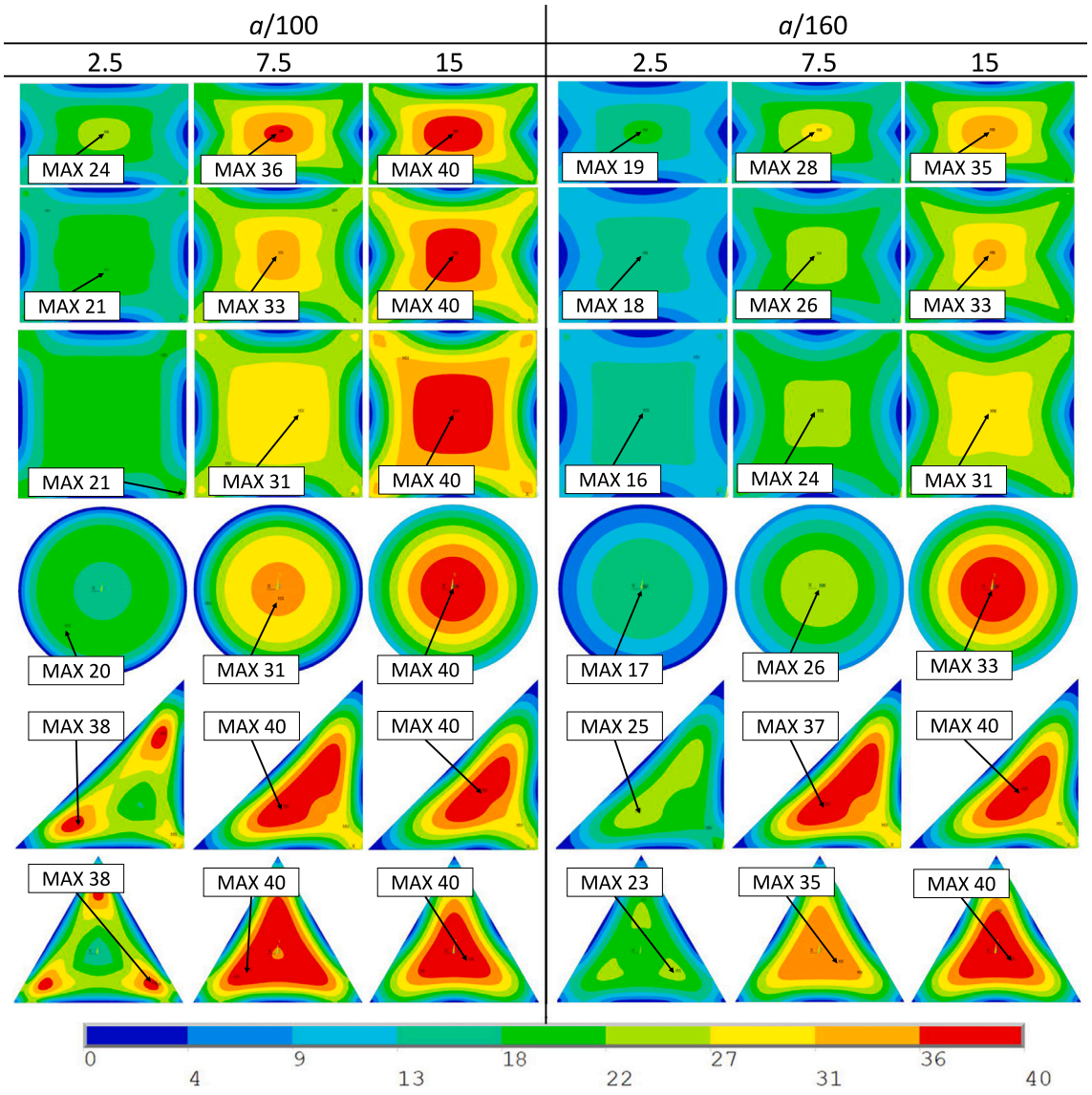

Fig. 16. The maximum principal stress contour plot of bottom of the exposed pane for all the shapes and design loads, and both deflection limits. The characterize length of $a = 3000$ mm is used. The legend range is the same for all, and the unit is MPa.

Next, the maximum normal stress components σ_x and σ_y, and the shear stress σ_{xy} in the exposed pane are extracted at the bottom surface and in the mid-plane. The value at the surface is the bending component of the stress while the value at the middle is membrane (the von Kármán) component. These are taken as the maximum values, regardless of their plane-wise location. Therefore, they may not be in the same location as the maximum value of the maximum principal stress. For brevity, only the smallest and the largest design loads are considered subjected to $a/100$ deflection limit. The results are presented in Table 5.

The ratio of the MID/BOT decreases as the load is increased. That is, when the glass panes are thicker, more load is carried through the bending. The same can be said when deflection limit is increased (not shown in the table). With smaller load and thinner glass panes, the membrane part is more active. However, since the boundary conditions in Fig. 3 allow for the in-plane movement of the edges and hence do not give "support" for resisting the stretching of the mid-plane, the membrane stress development is hindered. If the in-plane movement would be restricted, the von Kármán strains would be significantly greater. However, such boundary condition is not realistic with glass panes, and do not agree with experimental results, as shown in [11].

The bending and membrane stresses are higher in the triangular shapes than in the others for the smaller design load. This is the direct consequence of the deflection limit, which is more favorable for the triangles. On the other hand, the ratio of the MID/BOT stresses is the highest for the circular and square shapes for 2.5 kPa and 15.0 kPa design loads, respectively. However, there is not significant difference between the shapes for the ratios, except for the rectangles where the membrane part in the shorter side

Table 5
Stress components of the optimized thicknesses with $a = 3000$ mm subjected to $a/100$ deflection limit. These are the maximum values found in the exposed pane regardless of the plane-wise location. The BOT and MID values are taken at the bottom and at the middle of the shell element, respectively. The load is given in kPa and stresses in MPa.

Load	Shape	Loc	σ_x	σ_y	σ_{xy}	Load	Shape	Loc	σ_x	σ_y	σ_{xy}
2.5	R1.67	MID	4.5	1.2	1.6	15	R1.67	MID	2.9	0.9	1.0
		BOT	15.2	23.8	15.1			BOT	21.8	39.9	21.9
		MID/BOT	29.2%	4.9%	10.3%			MID/BOT	13.1%	2.1%	4.3%
	R1.25	MID	5.6	3.0	2.6		R1.25	MID	4.7	2.9	2.1
		BOT	18.4	20.6	17.2			BOT	31.1	40.0	26.9
		MID/BOT	30.3%	14.4%	15.0%			MID/BOT	15.1%	7.2%	7.7%
	S	MID	5.3	5.3	3.4		S	MID	6.1	6.1	3.4
		BOT	20.3	20.3	19.7			BOT	40.0	40.0	32.0
		MID/BOT	26.3%	26.3%	17.2%			MID/BOT	15.2%	15.2%	10.7%
	C	MID	6.5	6.5	7.7		C	MID	5.4	5.4	4.2
		BOT	20.1	20.1	5.2			BOT	39.6	39.6	7.2
		MID/BOT	32.3%	32.3%	147.5%			MID/BOT	13.6%	13.6%	59.2%
	T90	MID	8.7	8.7	8.8		T90	MID	3.1	3.1	3.4
		BOT	35.2	35.2	30.4			BOT	36.4	36.4	26.4
		MID/BOT	24.6%	24.6%	28.9%			MID/BOT	8.5%	8.5%	12.7%
	T60	MID	8.8	10.4	8.6		T60	MID	4.1	4.2	3.7
		BOT	37.9	34.1	19.5			BOT	39.4	38.8	17.3
		MID/BOT	23.1%	30.5%	44.0%			MID/BOT	10.3%	10.7%	21.6%

Abbreviations: "R" is rectangle, "S" is square, "C" is circle, and "T" is triangle.

direction diminishes as the aspect ratio is increased. There, the shorter side carries more load than the longer side, but through bending.

3.11. Comments on PSO

The implemented PSO algorithm performs well. Initially, a swarm size of 50 was chosen, as was done in [13]. However, extracting the response revealed that it had not converged to the optimum. Therefore, the swarm was increased to 150, which was sufficient to find the optimum. This optimum was generally found in less than 15 iterations, including the 4 consecutive iterations were no improvements were found. See Fig. 17 for an example. On the plotted domain, it can be seen that there is not much difference between cases where the thickness ratio is close to 1 and when it is at its maximum, 3. The figure also shows that continuous thickness values were used. In reality, the available thicknesses are discrete numbers with some interval. Using the real available thicknesses and IGUs with two glass panes, one could simply enumerate the results and the PSO would be too "advanced". However, when the number of variables increase, the number of possible variations increases exponentially. Indeed, the intention is to include the spacer thickness, and other variables in the future to find the optimum. Then, the PSO is well justified.

4. Discussion

It is clear that the weight of the insulating glass unit in modern cruise ships has become a problem to the shipbuilders. The reason for this is the increased usage of the IGUs whose behavior is not yet considered to their full potential in the classification rules. They provide easy-to-use equations for the thickness determination which provide a safe structure. This approach is good for passenger ships where the number of the IGUs is relatively small, but when lightweight solutions are sought for the state-of-the-art cruise ships, too much conservatism in the design leads to additional weight. While the result in [11] showed that the thickness of the glass panes in the IGUs may be decreased, it still did not give a comprehensive view of the cases that are present in the cruise ships. That is, it was limited to equally thick IGUs with rectangular shape. Therefore, it was not clear how the response changes when these limitations are removed. The purpose of this paper was indeed to shed light to this design space and demonstrate how one's decisions in the IGU design affect the thicknesses; the weight.

For this, the particle swarm optimization routine was used. Considering the study in this paper, it was probably too "advanced" algorithm, but it becomes necessary when more variables are added. In fact, when the optimization is done to insulating glass units consisting of laminated glasses, the number of variables can easily reach up to 7. Then, enumerate is not an option and it is very difficult to say whether the domain is concave, i.e., if gradient based methods would work. Furthermore, it is possible to include multiple objectives in the PSO, e.g., the thermal and noise insulation performance in addition to the structural performance. Therefore, PSO is a good choice. The implemented FE model in the optimization routine is very fast most of the times. Typically, one analysis only takes some 5 to 20 s, but when the area of the IGU is large and the thickness is small, the runtime may be even as high as 1 to 2 min. This is due to the geometrically nonlinear analysis. However, the nonlinear analysis is justified as described in [11]. The results that the optimization routine produced, were a little bit unexpected.

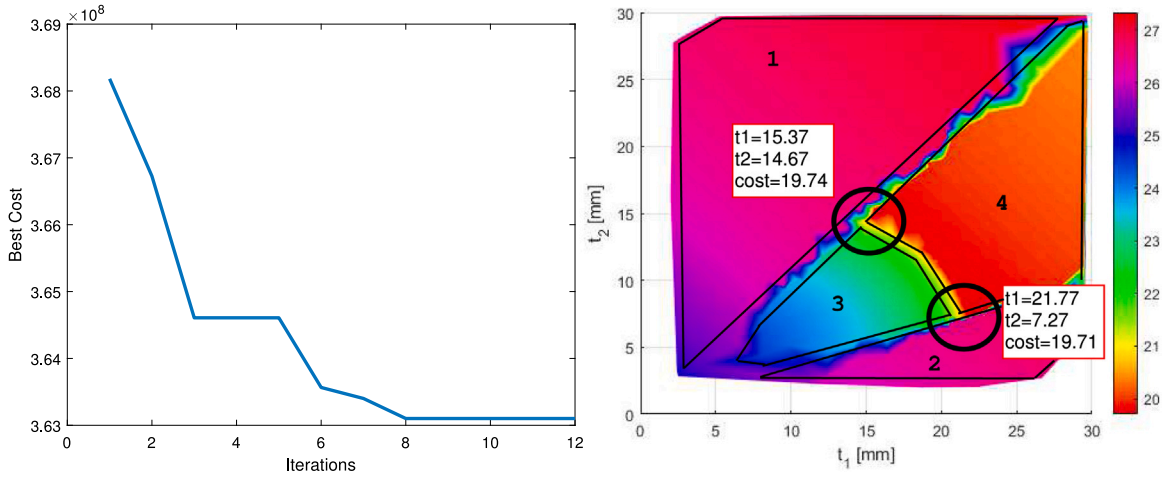

Fig. 17. An example of the convergence of the PSO algorithm on the left-hand side. On the right-hand side, is an example of the domain of the results. The cost represents the weight in both figures (lower is better). The numbers 1, 2, and 3 represents the unfeasible regions due to thickness ratios smaller than 1, thickness ratios larger than 3, and exceeding the other design constraints, respectively. The area within 4 is the feasible region. The costs 19.74 and 19.71 are the local and global optimums, respectively.

This is because in the earlier study, the load sharing and the geometric linearity were significant when the panes were equally thick.[5] It was an assumption that the optimization will further emphasize this. However, the optimum was found in the opposite direction, where the thickness of the exposed pane and the unexposed pane were made as thick as possible and as thin as possible, respectively. Hence, the thickness ratio was maximized. As a consequence, the load sharing percentage dramatically drops. This is because thick panes tend to deflect less, which hinders the internal pressure generation. The same applies to the von Kármán strains; thicker the pane is, more load is carried through bending. On the other hand, when the design is limited by the deflection, it is intuitive to minimize the deflection by introducing thick panes. However, the same trend was observed when the stresses are the limiting constraints. That is, regardless of the limiting constraints, the optimum is at a high thickness ratio number.

It is unclear what kind of thickness ratios are accepted, or suggested. Higher it is, more weight can be saved. However, the degree of redundancy drops at the same time. The difference between optimums at thickness ratios 1 and 3 is not very large (e.g., 10% for a square with $a = 3$ m). Therefore, it may be the best to choose something in between, where good redundancy and weight savings are achieved (e.g., between 1.5 and 2). Similar to the thickness ratio, it is not clear what kind of deflection limits should be used, or if they should be used at all. As of now, there is not enough information to give such recommendation. Future experiments will hopefully provide some of this information. However, the result show that even with the unequal thicknesses, the optimum thicknesses are sensitive to the chosen limit. Going higher limit decreases the load sharing and the von Kármán strains. The higher limit of $a/160$ is probably too conservative, since it produces thicknesses that have safety factor around 8 with respect to the strength for the smallest design load. And even the smallest load is rather high in magnitude, which is not encountered often in the top structures. Even if they would, the results in Fig. 15 show that IGUs optimized for 2.5 kPa design load with $a/100$ deflection criterion can easily withstand more than that.

The classification rules give thickness determination for all the considered shapes in this study except for the isosceles right triangle. For that, an equivalent dimension was established so the comparison could be made. Indeed, the triangular shapes enjoy the most lightweight design. They have the least weight for a given area in most of the cases. This is partly due to the imposed deflection limits, that are favorable for these shapes. Closer the stress is to the design limit, the smaller the differences get. Usually, triangular shapes are very popular in cruise ships because it easy to make curved surfaces (domes) with them. However, this means that if they are designed according to the class rules, they are the worst when it comes to having a lightweight design. That is, there is the most savings available with the triangular shapes. Considering the most common case, i.e., small design load, with the $a/100$ deflection limit, circular shape also provide large potential savings. There is not much difference among the rectangular shapes.

However, when the support structure between the IGUs is included, the differences between the shapes change. The square IGUs can be the lightest (depending on the steel support profile) for small side lengths, while the triangular shapes are the lightest with large side lengths. If a wall between decks is covered with windows, deck height being about 2.3 to 3 m, then there is not much difference whether the shape is rectangular or triangular, from the weight perspective. So, other design criteria may dictate the decision, such as e.g., aesthetical or structural. The story is different for the large glass structures, e.g., domes or other glass

[5] An interested reader is referred to Table 5 and Figure 17 in [11] to see how the geometric nonlinearity and the load sharing affect the weight separately and together, and how they reflect on the classification rules.

ceilings, whose steel structures are typically disjointed to some degree from the ship's global response. Furthermore, they are often located on the top structures. Hence, the glass weight optimization may be more important for those than of those located between the decks.

Finally, from the obtained optimized thicknesses, it is clear that they increase linearly as the side length (or diameter) is increased for a given design load. Meaning that it would be possible in theory to establish a simple linear equation for the thickness determination of these shapes that would take into account the load sharing, the geometric nonlinearity, and the presented boundary condition. However, such formulation would require more in depth study of the different cases, and a dialogue with the different parties. But in the meanwhile, determining the thickness of the glass panes using FE method is the suggested way.

5. Conclusions

The paper studied numerically how the different design criteria affect the thickness determination of the glass pane in the insulating glass units (IGUs) used in cruise ships. Six different IGU shapes were studied using the nonlinear finite element method and particle swarm optimization; rectangular ($a/b = 1$, $a/b = 1.25$, $a/b = 1.67$), triangular (right angle and equilateral), and circular. These represents some of the elementary shapes that can be currently found in cruise ships. The goal was to give insight on how to achieve the lightweight design and provide reasoning for it.

The most influencing design criterion on the behavior of the IGU was the thickness ratio between the glass panes (t_1/t_2). Closer the panes are to equal thickness, more even the response is between the glass panes. However, the most weight can be saved when the thickness ratio is high. Then, the load is carried mostly by the thicker glass pane through bending. The deflection criterion also has a significant influence on the response. In most cases, it dominated over the stress criterion resulting in additional weight. The IGU shape also plays an important role in the design. In this study, the triangular shapes could provide the least weight for a given area. However, there are good potential weight savings for all the shapes with respect to the classification rules for moderate sizes, even with imposed deflection criterion.

This study neglected dynamic loading and laminated glasses. IGUs closer to the sea level may be subjected to water induced loading and hence quasi-static analysis is not a good presentation. However. it is not clear how the load sharing is affected by the dynamic loading. Laminated glasses are used in places where broken shards may pose harm to the passengers. In fact, many of the IGUs are indeed laminated glasses. Finally, the usage of the deflection limit in the design requires further attention. That is, how the IGUs behave under large deflections. Therefore, the intention is to study all of these in the future, numerically and experimentally.

Declaration of competing interest

The authors declare that they have no known competing financial interests or personal relationships that could have appeared to influence the work reported in this paper.

Data availability

Data will be made available on request.

Acknowledgments

The corresponding author was supported by the School of Engineering at Aalto University, Finland. Further, the research presented in this paper has received funding from Business Finland under grant No. 3409/31/2022. The work is part of the Carbon neutral lightweight ship structures using advanced design, production, and life-cycle Services (CaNeLis) project within the scope of Climate-Neutral Cruise Ship (NEcOLEAP) and Sustainable Manufacturing Finland roadmaps. All financial support is gratefully appreciated. Finally, Ari Niemelä, head of hull basic design at Meyer Turku Oy, is greatly acknowledged for providing helpful comments and feedback.

Appendix A. Determination of glass pane thickness according to classification rules

The classification rules provide thickness determination for rectangular and circular windows. The thickness for equilateral triangle is calculated using equivalent dimensions. However, there is no equation for the isosceles right angle triangle, but one can be established by using the equivalent dimension method. These are presented next according to ISO 11336-1 [27] standard, which is equivalent to DNV [12], Lloyd's Register [29], and Bureau Veritas [30] methods. That is, they all use linear plate theory with maximum principal stress criterion. The strength of fully tempered glass is given as 160 MPa, and with safety factor of 4, the design strength is 40 MPa.

For rectangular pane, the required thickness, t_r, is dependent on the design load, p_d, the shorter side length, b, the aspect ratio factor, β, which is dependent on the aspect ratio, a/b, and given by the rule or standard, and the design flexural strength, σ_d. Then, the thickness is:

$$t_r = b\sqrt{\frac{\beta p_d}{1000\sigma_d}} \tag{A.1}$$

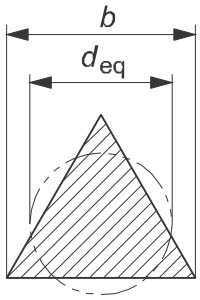

Fig. A.18. Equivalent diameter for equilateral triangle.

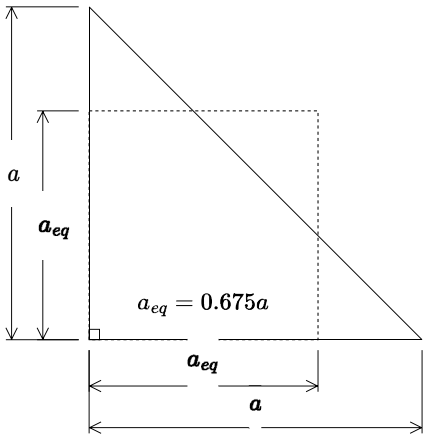

Fig. A.19. Equivalent diameter for isosceles right triangle.

For circular pane, the equation is practically the same, but with diameter, d, and without the aspect ratio factor:

$$t_r = 0.5d\sqrt{\frac{1.21p_d}{1000\sigma_d}} \tag{A.2}$$

Equivalent diameter, d_{eq}, must be calculated for the equilateral triangle (see Fig. A.18). That is given by $d_{eq} = 3b/4$. Then the thickness is simply calculated as for the circular pane.

Similar must be done with isosceles right triangle (see Fig. A.19). The equivalent dimension is $a_{eq} = 0.675a$, which is determined by the author by using linear finite element analysis, so that the maximum principal stress for the triangle becomes 40 MPa for the respective load. Then, one can calculate the required thickness using the rectangular equation in Eq. (A.1) with $a/b = 1$ ($\beta = 0.2874$).

While there are thickness determination rules for collaborating glass panes, it only considers laminated glasses. No insulating glass units are considered in the rules, besides for Bureau Veritas [30]. It states for "Thickness of double windows": "The thickness of the ply exposed to the loads defined in [3.3.2] is to be calculated as per monolithic windows according to [3.3.4]". The [3.3.4] refers to what is shown in Eq. (A.1), and [3.3.2] is defining the design load, not shown in this paper. This means that there is no design rule for the unexposed pane.

Appendix B. The full figures

See Figs. B.20–B.26.

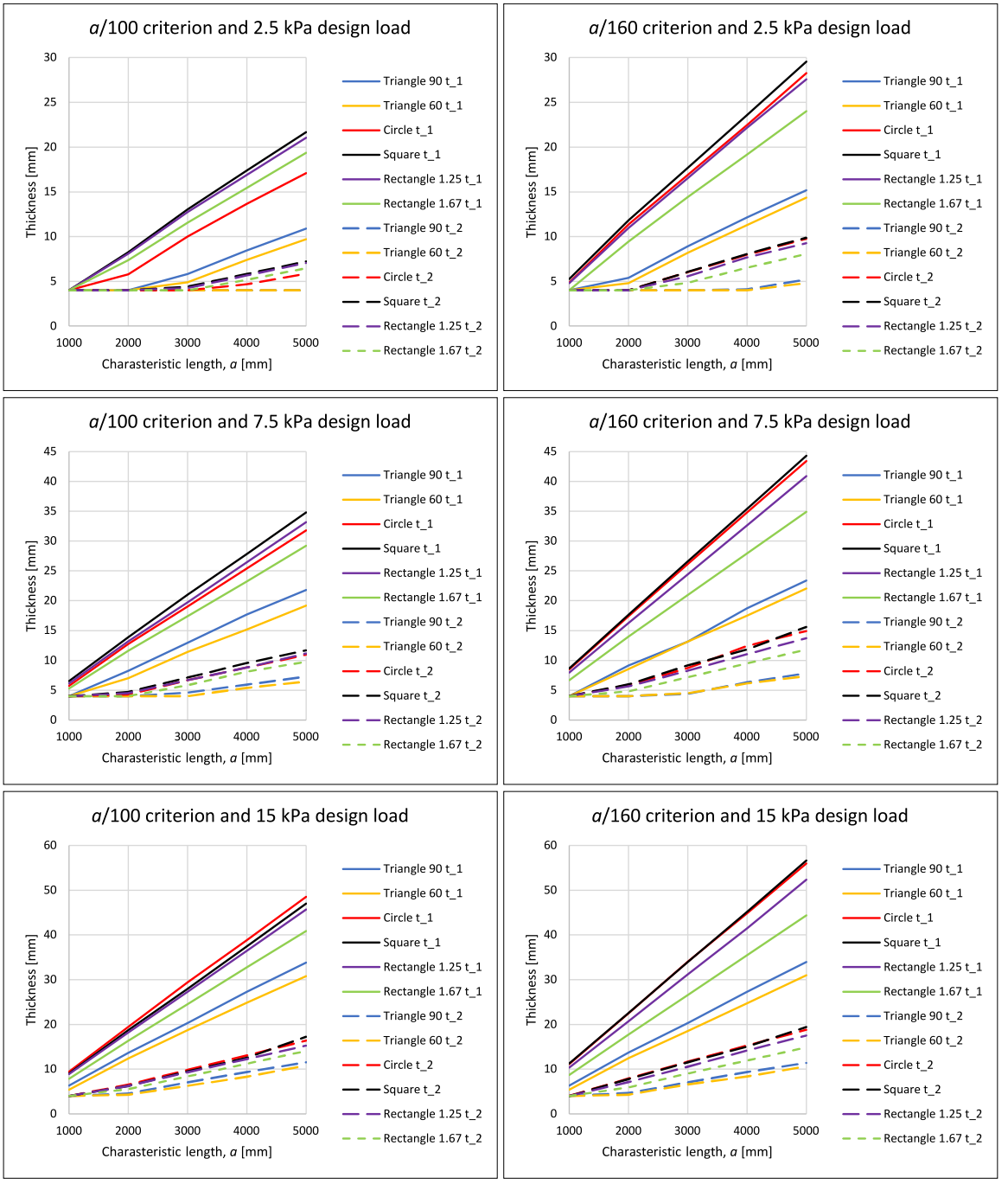

Fig. B.20. The optimized thicknesses: t_1 and t_2 are for exposed pane and unexposed pane, respectively.

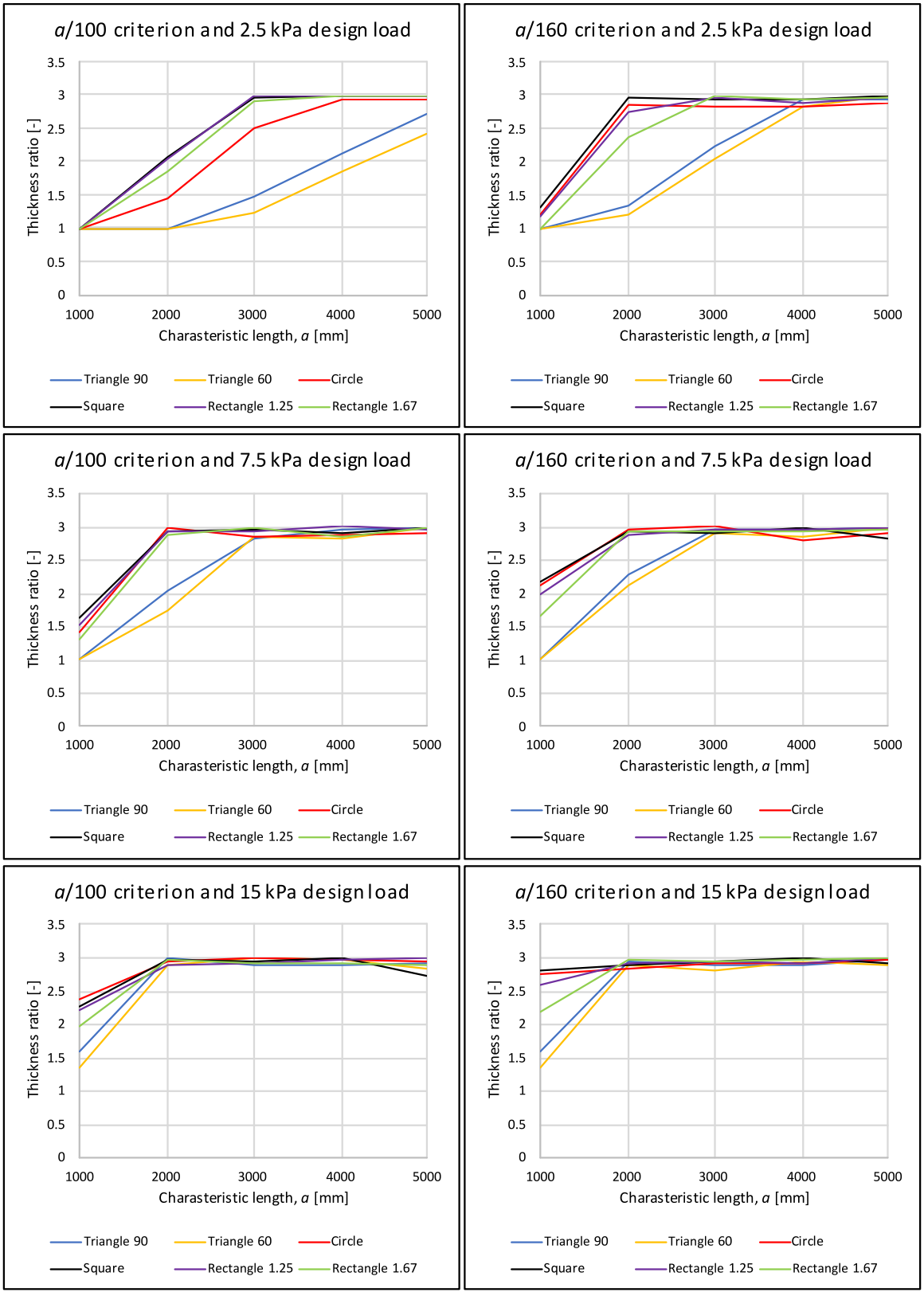

Fig. B.21. The thickness ratio of exposed pane to unexposed pane for the optimized thicknesses.

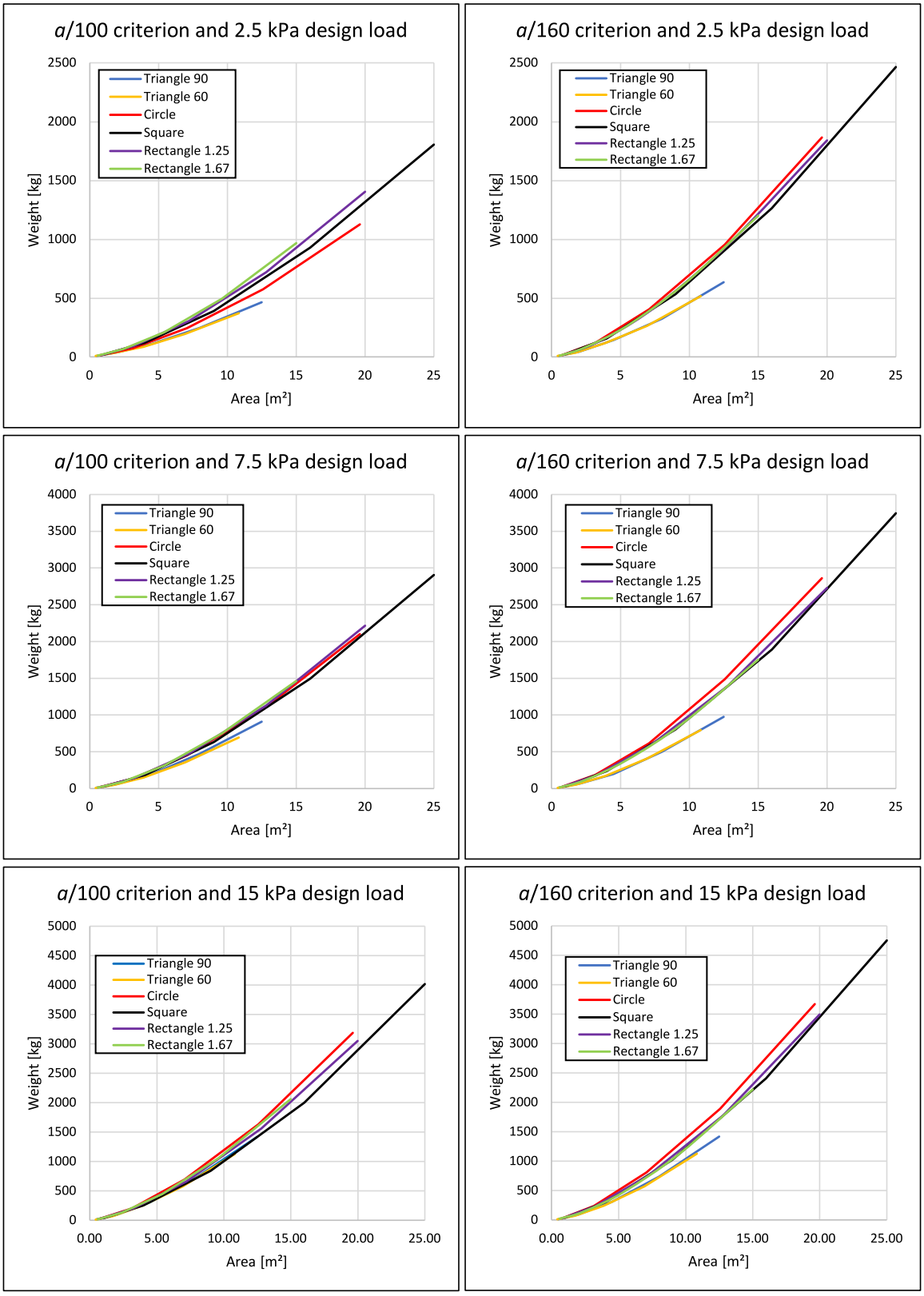

Fig. B.22. Weight vs. area comparison of the optimized thicknesses.

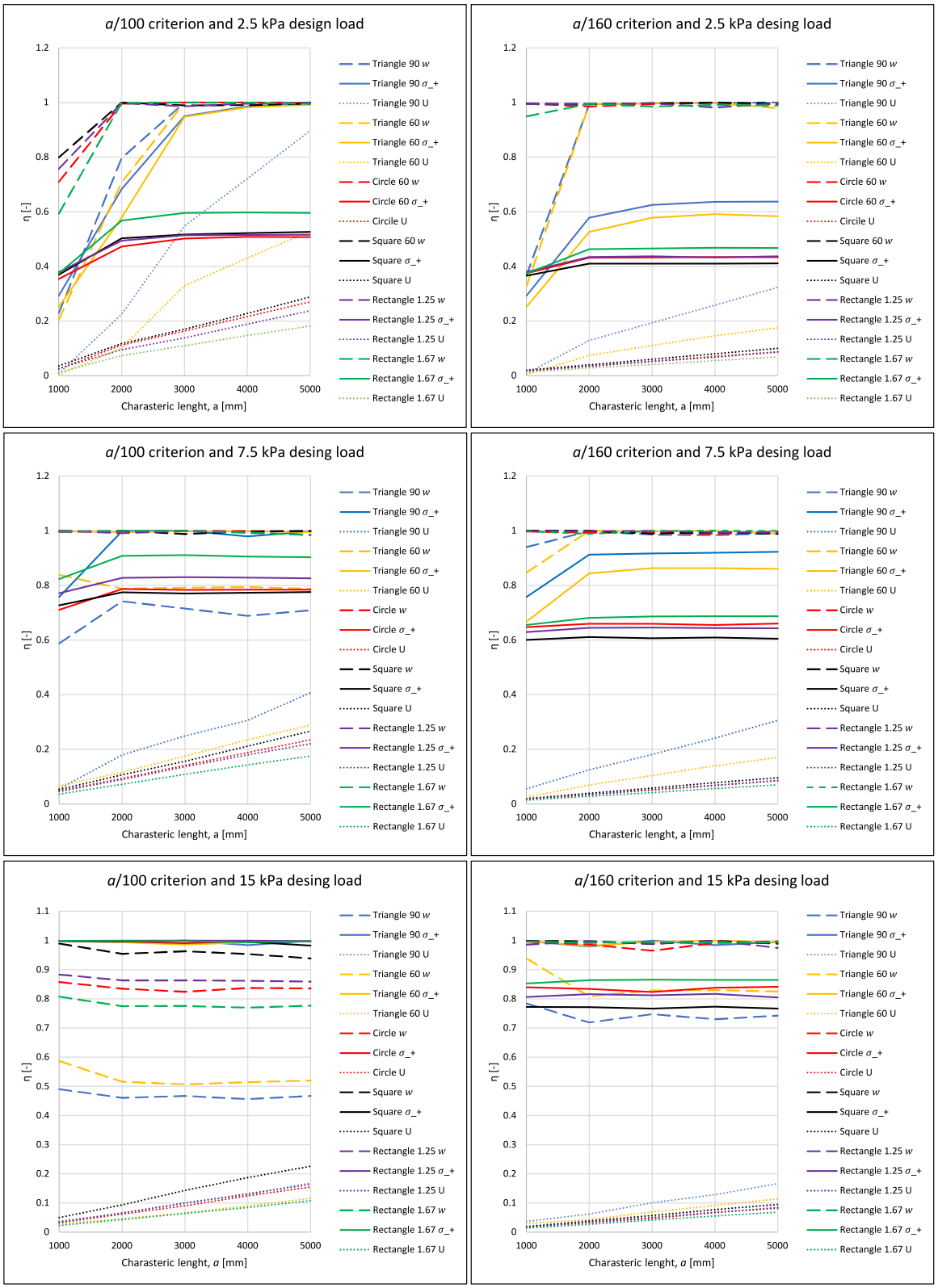

Fig. B.23. Activation of the design criteria in the exposed pane. The activation is $\eta = response/criterion$. Value of 1 means that the criterion has been reached. U is the maximum in-plane translation of the edge and w is maximum the deflection as shown in Fig. 3, and σ_+ is the maximum principal stress.

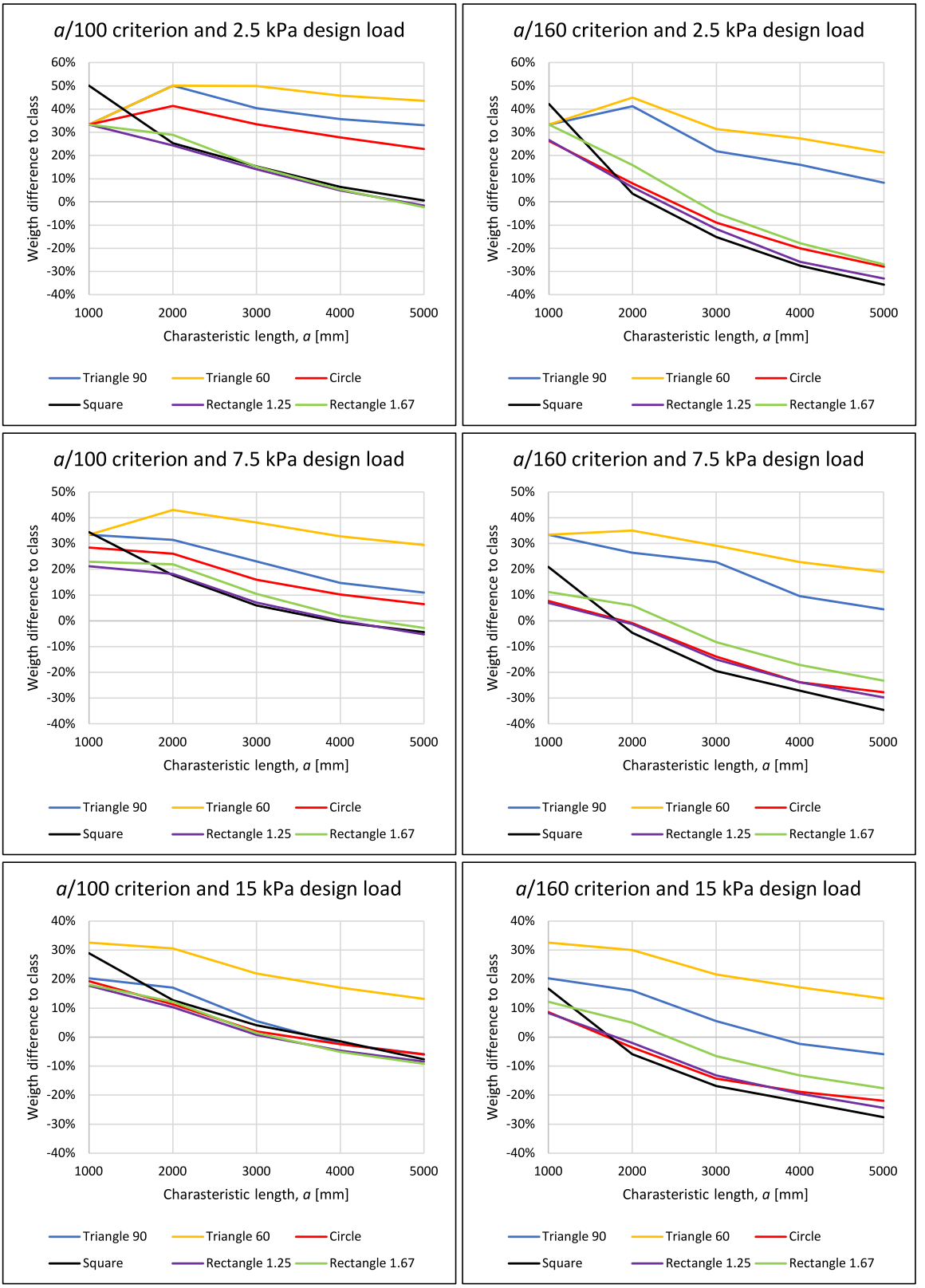

Fig. B.24. Weight difference between the optimized thickness and the classification society method as per ISO 11336-1 [27]. The optimized thicknesses follow $t_1 \neq t_2$, while the classification thicknesses follow t_1 according to equations in Appendix A (minimum 6 or 8 mm), and t_2 is 6 mm if less than 1 m^2 or 8 mm otherwise.

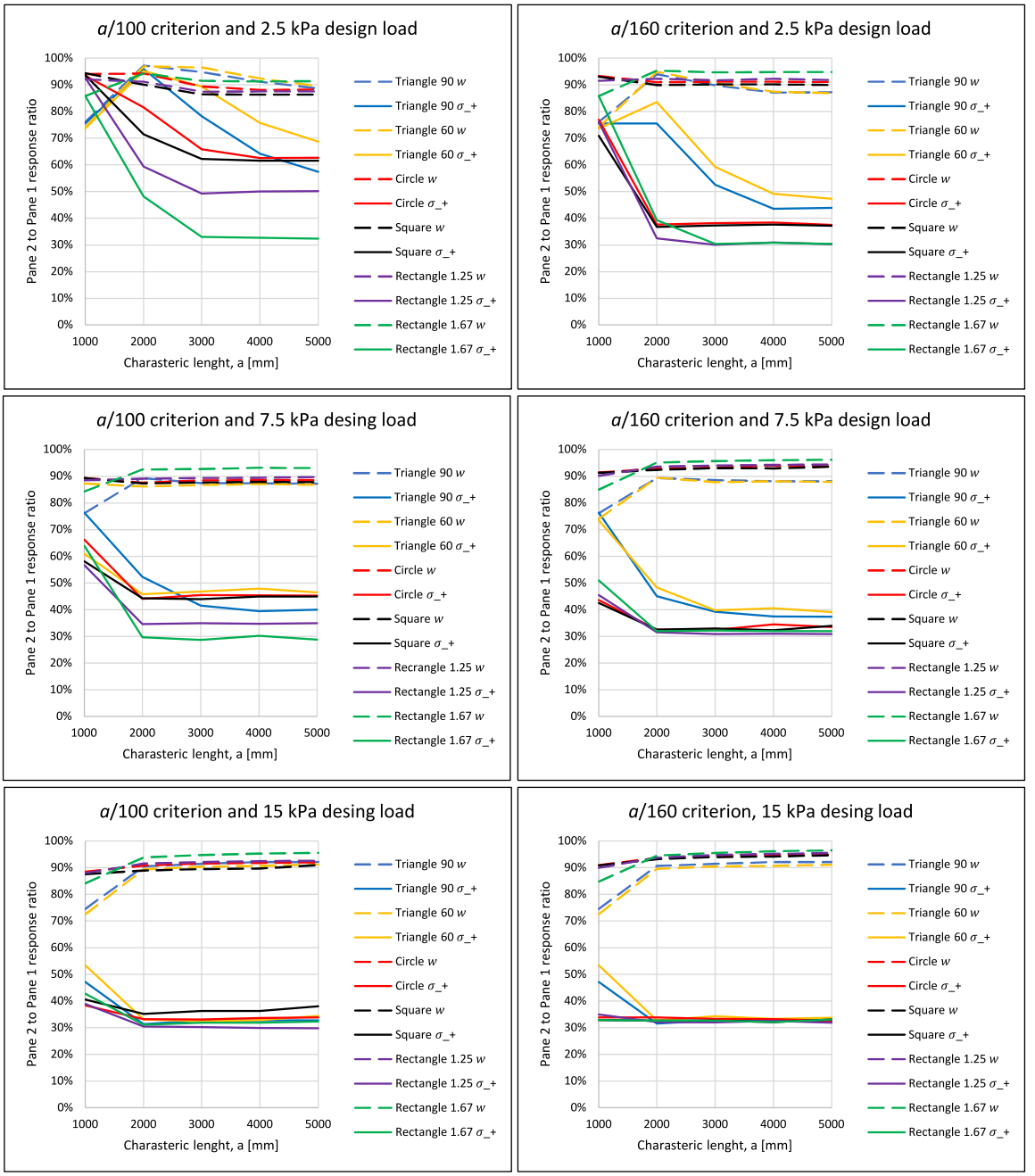

Fig. B.25. The response ratio between unexposed pane (pane 2) and the exposed pane (pane 1). 100% means that the panes have identical response. σ_+ is the maximum principal stress, and w is the deflection.

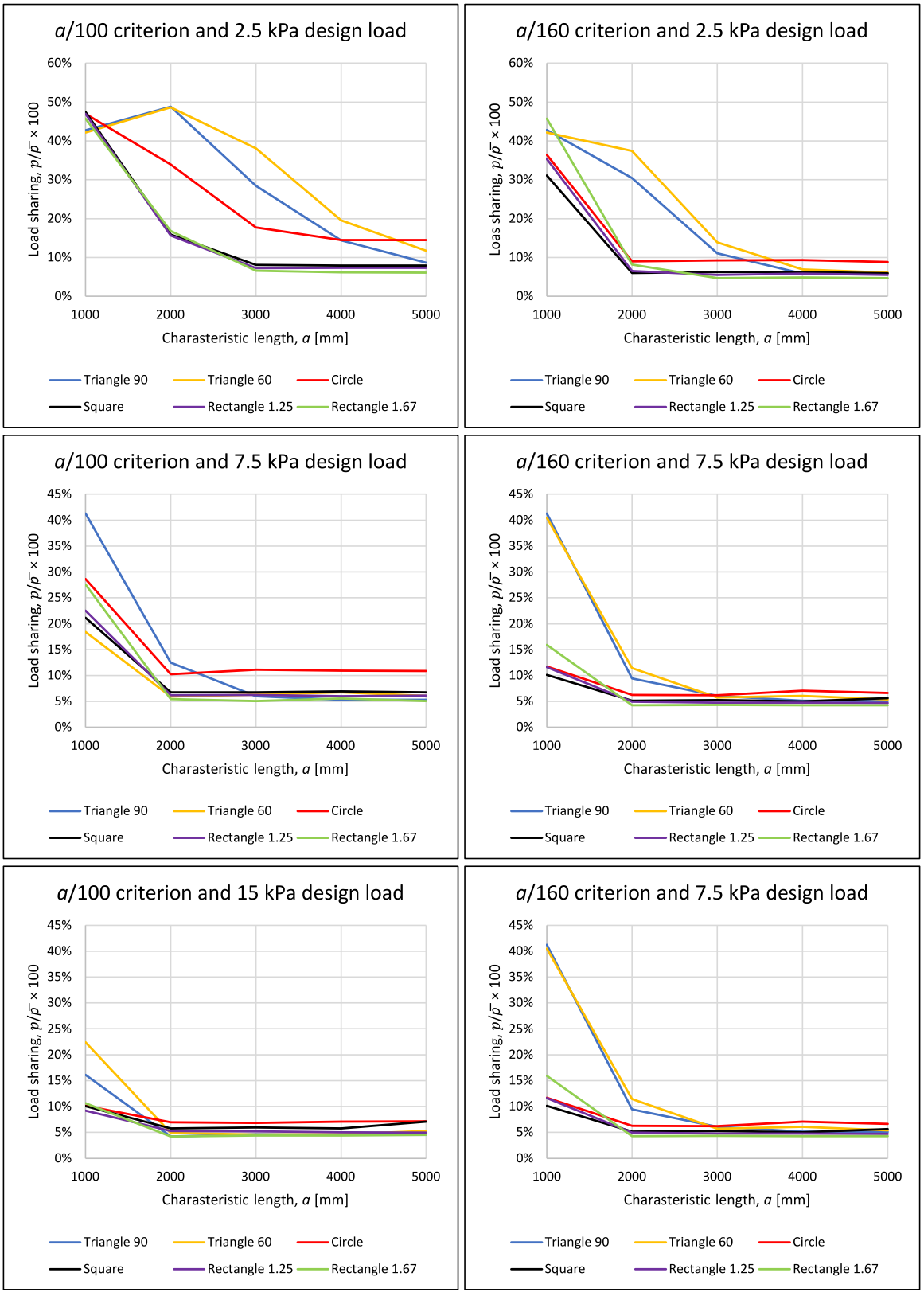

Fig. B.26. Load sharing between the panes. It is calculated as the ratio of the pressure inside the cavity and the applied external pressure.

References

[1] Lillemäe I, Remes H, Romanoff J. Influence of initial distortion of 3 mm thin superstructure decks on hull girder response for fatigue assessment. Mar Struct 2014;37:203–18. http://dx.doi.org/10.1016/j.marstruc.2014.04.001, URL http://www.sciencedirect.com/science/article/pii/S095183391400029X.

[2] Jelovica J, Romanoff J, Klein R. Eigenfrequency analyses of laser-welded web–core sandwich panels. Thin-Walled Struct 2016;101:120–8. http://dx.doi.org/10.1016/j.tws.2016.01.002, URL https://www.sciencedirect.com/science/article/pii/S0263823116300027.

[3] Crupi V, Epasto G, Guglielmino E. Comparison of aluminium sandwiches for lightweight ship structures: Honeycomb vs. foam. Mar Struct 2013;30:74–96. http://dx.doi.org/10.1016/j.marstruc.2012.11.002, URL http://www.sciencedirect.com/science/article/pii/S0951833912000810.

[4] Avi E, Laakso A, Romanoff J, Remes H, Lillemäe-Avi I. Coarse mesh finite element model for cruise ship global and local vibration analysis. Mar Struct 2021;79:103053. http://dx.doi.org/10.1016/j.marstruc.2021.103053, URL https://www.sciencedirect.com/science/article/pii/S0951833921001088.

[5] Heder M, Ulfvarson A. Hull beam behaviour of passenger ships. Mar Struct 1991;4(1):17–34. http://dx.doi.org/10.1016/0951-8339(91)90022-4, URL https://www.sciencedirect.com/science/article/pii/0951833991900224.

[6] Wiegard B, Ehlers S, Klapp O, Schneider B. Bonded window panes in strength analysis of ship structures. Ship Technol Res 2018;65(2):102–21. http://dx.doi.org/10.1080/09377255.2018.1459066.

[7] Gerlach B, Fricke W. Experimental and numerical investigation of the behavior of ship windows subjected to quasi-static pressure loads. Mar Struct 2016;46:255–72. http://dx.doi.org/10.1016/j.marstruc.2016.02.001, URL https://www.sciencedirect.com/science/article/pii/S095183391600006X.

[8] McMahon S, Scott Norville H, Morse SM. Experimental investigation of load sharing in insulating glass units. J Archit Eng 2018;24(1):04017038.

[9] Galuppi L, Royer-Carfagni G. Betti's Analytical Method for the load sharing in double glazed units. Compos Struct 2020;235:111765. http://dx.doi.org/10.1016/j.compstruct.2019.111765, URL http://www.sciencedirect.com/science/article/pii/S0263822319325541.

[10] Respondek Z, Kozłowski M, Wiśniowski M. Deflections and stresses in rectangular, circular and elliptical insulating glass units. Materials 2022;15(7):2427.

[11] Heiskari J, Romanoff J, Laakso A, Ringsberg JW. On the thickness determination of rectangular glass panes in insulating glass units considering the load sharing and geometrically nonlinear bending. Thin-Walled Struct 2022;171:108774. http://dx.doi.org/10.1016/j.tws.2021.108774, URL https://www.sciencedirect.com/science/article/pii/S0263823121007631.

[12] DNV, rules for classification: Ships, part 3 hull, chapter 12 openings and closing appliances. July ed. L; 2022.

[13] Heiskari J, Romanoff J, Laakso A, Ringsberg JW. Thickness optimization of insulating glass unit in cruise ships. In: Practical design of ships and other floating structures. 2022, p. 910–24.

[14] Buddenberg S, Hof P, Oechsner M. Climate loads in insulating glass units: comparison of theory and experimental results. Glass Struct Eng 2016;1(1):301–13. http://dx.doi.org/10.1007/s40940-016-0028-z.

[15] Kozłowski M, Respondek Z, Wiśniowski M, Cornik D, Zemła K. Experimental and numerical simulations of climatic loads in insulating glass units by controlled change of pressure in the gap. Appl Sci 2023;13(3):1269.

[16] Bao M, Gregson S. Sensitivity study on climate induced internal pressure within cylindrical curved IGUs. Glass Struct Eng 2019;4(1):29–44.

[17] Heiskari J. On the design criteria of large insulating glass structures in cruise ships [Master's thesis], Aalto University and Chalmers University of Technology; 2020.

[18] DIN 18008-1:2010-12 - Glass in building - Design and construction rules - Part 1: Terms and general bases.

[19] Raikunen J, Avi E, Remes H, Romanoff J, Lillemäe-Avi I, Niemelä A. Optimisation of passenger ship structures in concept design stage. Ships Offshore Struct 2019;14(sup1):320–34. http://dx.doi.org/10.1080/17445302.2019.1590947.

[20] Romanoff J. Optimization of web-core steel sandwich decks at concept design stage using envelope surface for stress assessment. Eng Struct 2014;66:1–9. http://dx.doi.org/10.1016/j.engstruct.2014.01.042, URL https://www.sciencedirect.com/science/article/pii/S014102961400056X.

[21] Bedon C, Amadio C. Mechanical analysis and characterization of IGUs with different silicone sealed spacer connections-Part 2: Modelling. Glass Struct Eng 2020;5(3):327–46.

[22] Piotrowski AP, Napiorkowski JJ, Piotrowska AE. Population size in particle swarm optimization. Swarm Evol Comput 2020;58:100718. http://dx.doi.org/10.1016/j.swevo.2020.100718, URL https://www.sciencedirect.com/science/article/pii/S2210650220303710.

[23] He M, Liu M, Wang R, Jiang X, Liu B, Zhou H. Particle swarm optimization with damping factor and cooperative mechanism. Appl Soft Comput 2019;76:45–52. http://dx.doi.org/10.1016/j.asoc.2018.11.050, URL https://www.sciencedirect.com/science/article/pii/S1568494618306823.

[24] Freitas D, Lopes LG, Morgado-Dias F. Particle swarm optimisation: A historical review up to the current developments. Entropy 2020;22(3). http://dx.doi.org/10.3390/e22030362, URL https://www.mdpi.com/1099-4300/22/3/362.

[25] EN 12600:2002 Glass in building - Pendulum test - Impact test method and classification for flat glass.

[26] EN 1288-3:2000 Glass in building - Determination of the bending strength of glass - Part 3: Test with specimen supported at two points (four point bending).

[27] ISO 11336-1:2012, Large yachts - Strength, weathertightness and watertightness of glazed openings - Part 1: Design criteria, materials, framing and testing of independent glazed openings. Geneva: International Organization for Standardization.

[28] Gerlach B, Fricke W, Guiard M, Ferreira González D, Abdel-Maksoud M. Failure prediction of ship windows subjected to wave impacts. Ship Technol Res=Schiffstechnik 2015;62(3):159–72.

[29] Lloyd's register, rules and regulations for the classification of ships, July. 2022.

[30] Bureau Veritas, rules for the classification of steel ships, Part B hull and stability, July. 2022.